DO I LOOK LIKE A "CAT.N.01" TO YOU? A TAXONOMY IMAGE GENERATION BENCHMARK

Anonymous authors
Paper under double-blind review

ABSTRACT

This paper explores the feasibility of using text-to-image models in a zero-shot setup to generate images for taxonomy concepts. While text-based methods for taxonomy enrichment are well-established, the potential of the visual dimension remains unexplored. To address this, we propose a comprehensive benchmark for Taxonomy Image Generation that assesses models' abilities to understand taxonomy concepts and generate relevant, high-quality images. The benchmark includes common-sense and randomly sampled WordNet concepts, alongside the LLM generated predictions. The 12 models are evaluated using 9 novel taxonomy-related text-to-image metrics and human feedback. Moreover, we pioneer the use of pairwise evaluation with GPT-4 feedback for image generation. Experimental results show that the ranking of models differs significantly from standard T2I tasks. *Playground-v2* and *FLUX* consistently outperform across metrics and subsets and the retrieval-based approach performs poorly. These findings highlight the potential for automating the curation of structured data resources.

1 INTRODUCTION

In recent years, Large Language Models (LLMs) and Visual Language Models (VLMs) have demonstrated remarkable quality across a wide range of single- and cross-domain tasks Esfandiarpoor et al. (2024); Esfandiarpoor & Bach (2023); Du et al. (2023); Jiang et al. (2024b). Their capabilities also expand to the tasks traditionally dominated by human input, such as annotation and data collection Tan et al. (2024). At the very same time, the urge for manually created datasets and databases still remains popular, as more accurate and reliable Zhou et al. (2023), even though they are time-consuming and expensive to be kept up-to-date.

In this paper, we focus on taxonomies — lexical databases that organize words into a hierarchical structure of "IS-A" relationships. WordNet Miller (1998) is the most popular taxonomy for English, forming the graph backbone for many downstream tasks Mao et al. (2018); Lenz & Bergmann (2023); Fedorova et al. (2024). In addition to textual data, taxonomies also extend to visual sources, e.g. ImageNet Deng et al. (2009). ImageNet is built upon the WordNet taxonomy by associating concepts or "synsets" (sets of synonyms, aka lemmas) with thousands of manually curated images. However, it covers a very small portion of WordNet taxonomy (5,247 out of 80,000 synsets in total, 6.5%).

From the visual perspective, Text-to-Image models are widely used for the visualizations Ng et al. (2024); Sha et al. (2023), but only occasionally for taxonomies Patel et al. (2024a). Therefore, there is limited knowledge about how well text-to-image models are capable of visualizing concepts of different level of abstraction in comparison to humans Liao et al. (2024). Image generation for taxonomies could be quite specific and require additional research: Figure 1 highlights the key differences in prompt usage for the DiffusionDB dataset Wang et al. (2023) and WordNet-3.0. Moreover, the output taxonomy-linked depictions should aim succinctly portraying the synset's core idea and/or sometimes revealing insights about the concept that are challenging to convey textually.

Therefore, in this paper, we address this gap by investigating the use of automated methods for updating taxonomies in the image dimension (depicting). Specifically, we develop an evaluation benchmark comprising 9 metrics for Taxonomy Image generation using both human and automatic evaluation and a Bradley-Terry model ranking in line with recent top-rated evaluation methodology Chiang et al. (2024a); Zheng et al. (2023b). Suprisingly, our task yields different rankings for models

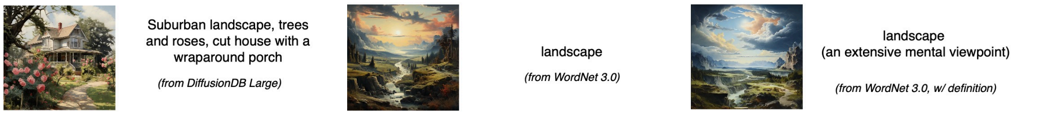
Suburban landscape, trees and roses, cut house with a wraparound porch
(from DiffusionDB Large)
landscape
(from WordNet 3.0)
landscape
(an extensive mental viewpoint)
(from WordNet 3.0, w/ definition)

Figure 1: Comparison of generations of the *Playground* model for the input prompt from the DiffusionDB dataset and available inputs from the WordNet-3.0. It can be seen, that the input from the TTI dataset is more detailed and the inner model representation could be misguiding even when the difinition is given.

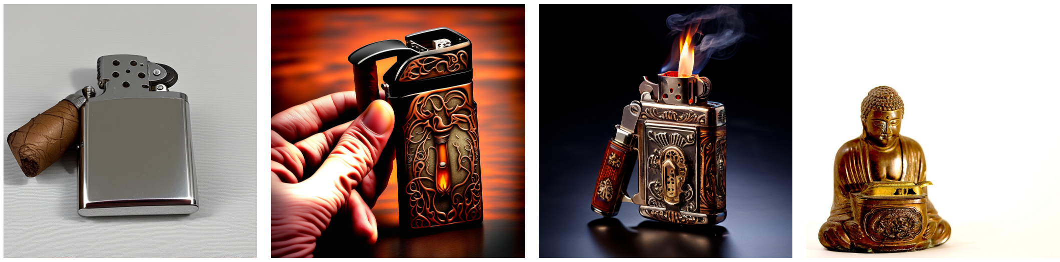
(a) Kandinsky 3 (b) SD3 (c) Playground (d) Retrieval

Figure 2: The example of a generation and retrieval results for *cigar lighter*. As can be observed, the generation approach is significantly superior to the retrieval approach, as the retrieved image is quite unconventional.

compared to those in text-to-image benchmarks Jiang et al. (2024a), higlighting the task importance. We also uncover that modern Text-to-Image models outperform traditional retrieval-based methods in covering a broader range of concepts, highlighting their ability to better represent and visualize these previously underexplored areas.

The contributions of the paper are as follows:

- We propose a benchmark comprising 9 metrics, including
  - several taxonomy-specific text-to-image metrics (grounded with theoretical justification drawing on KL Divergence and Mutual Information)
  - pairwise preference evaluation with GPT-4 for text-to-image generation and analyze its alignment with human preferences, biases, and overall performance.
- We test on the dataset specifically designed for Taxonomy Image Generation task, which presents challenges that were previously unaddressed in text-to-image research.
- We are the first to evaluate the performance of the 12 publicly available Text-to-Image models to generate images for WordNet concepts on the developed benchmark.
- We publish the dataset of the images generated by the best Text-to-Image approach from the benchmark that fully covers WordNet-3.0 extending the ImageNet dataset.

2 DATASETS

This section provides an overview of the datasets used to evaluate the performance of text-to-image (TTI) models. It includes the Easy Concepts dataset, the TaxoLLaMA test set derived from WordNet, and the predictions generated by the TaxoLLaMA model. The aim of the datasets is to assess the models' sensitivity to easier/harder dataset and to existing/AI-generated entities.

2.1 EASY CONCEPT DATASET

The Easy Concepts dataset from Nikishina et al. (2023) comprises 22 synsets selected by the authors as common-sense concepts (e.g. *"coin.n.01, chromatic_color.n.01, makeup.n.01, furniture.n.01"*, etc.). We extend this list by including their direct hyponyms ("children nodes"), following the methodology outlined in the original paper and based on the English WordNet (Miller, 1998). The resulting dataset comprises 483 entities and represents a broader set of common knowledge entities.

2.2 Random Split from WordNet

To generate the second dataset, we use the algorithm from TaxoLLaMA (Moskvoretskii et al., 2024b). We randomly sample the nodes the following types of hierarchical relations between synsets:

- **Hyponymy (Hypo)**: from a broader word (*“working_dog.n.01”*) to a more specific (*“husky.n.01”*). Here we take a broader word for image generation.
- **Hypernymy (Hyper)**: from a more specific word (*“capuccino.n.01”*) to a broader concept (*“coffee.n.01”*). Here we take a more specific word for image generation.
- **Synset Mixing (Mix)**: nodes created by mixing at least two nodes (e.g. *“milk.n.01”* is a *“beverage.n.01”* and a *“diary_product.n.01”*). Here we take the node created by mixing for depiction.

The algorithm for sampling uses a 0.1 probability for sampling Hyponymy, a 0.1 probability for sampling Synset Mixing, and a 0.8 probability for sampling Hypernymy. The dominance of Hypernymy is necessary because it is the most useful relation for training TaxoLLaMA Moskvoretskii et al. (2024a). To mitigate this bias, the probabilities of occurrence in the test set differ between cases: for Hypernymy is set very low at 1×10^{-5}, higher for Hyponymy at 0.05, and highest for Synset Mixing at 0.1, as these cases are rare.

The resulting test set includes 1,202 nodes: 828 from Hypernymy relations, 170 from Synset Mixing relations, and 204 from Hyponymy relations.

2.3 LLM Predictions Datasets

As our final goal is depicting of the new concepts for taxonomy extension, we should also test TTI models with LLM predictions rather than ground-truth synsets. Therefore, we finetune an LLM model on the Taxonomy Enrichment task to use its predictions and assess the sensitivity of text-to-image (TTI) models to AI-generated content.

The workflow comprises three steps: (i) exclude the Easy Concept dataset and random split from the overall WordNet data for LLM model training; (ii) train the updated version of TaxoLLaMA with LLaMA-instruct-3.1 Dubey et al. (2024); (iii) solve the Taxonomy Enrichment task for the test data to generate concepts for vizualization. When training the TaxoLLaMA-3.1 model, we follow the methodology outlined in Moskvoretskii et al. (2024b).

This process resulted in 1,685 items. To match the original WordNet synsets, we generate definitions for every generated node with GPT4, described in Appendix C.

3 Models

In this section, we describe ten TTI models and one Retrieval model (12 in total) and the details of image collection. Table 1 comprises the full list of the models compared in the evaluation benchmark, their description can be found in Appendix B.

An example of a prompt for image generation is demonstrated below, details are described in Appendix F. We perform experiments with two versions of the prompt: with and without definition. It is worth noting that adding definitions does not turn the task into “standard instruction following.” In TTI settings, definitions are not a typical or natural form of instruction, therefore it is an additional informative diagnostic, revealing how models retrieve fine-grained taxonomic meaning. Figure 2 shows the example of a generation and retrieval results guided by the prompt:

```
TEMPLATE: An image of <CONCEPT> (<DEFINITION>)

EXAMPLE: An image of cigar lighter (a lighter for cigars or
cigarettes)
```

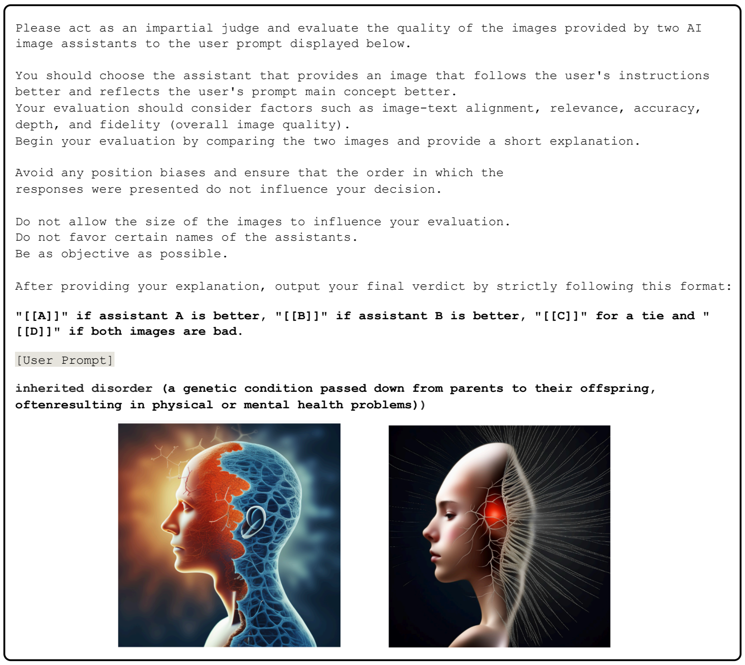

```
Please act as an impartial judge and evaluate the quality of the images provided by two AI
image assistants to the user prompt displayed below.

You should choose the assistant that provides an image that follows the user's instructions
better and reflects the user's prompt main concept better.
Your evaluation should consider factors such as image-text alignment, relevance, accuracy,
depth, and fidelity (overall image quality).
Begin your evaluation by comparing the two images and provide a short explanation.

Avoid any position biases and ensure that the order in which the
responses were presented do not influence your decision.

Do not allow the size of the images to influence your evaluation.
Do not favor certain names of the assistants.
Be as objective as possible.

After providing your explanation, output your final verdict by strictly following this format:

"[[A]]" if assistant A is better, "[[B]]" if assistant B is better, "[[C]]" for a tie and "
[[D]]" if both images are bad.

[User Prompt]

inherited disorder (a genetic condition passed down from parents to their offspring,
oftenresulting in physical or mental health problems))
```

Figure 3: LLM prompt example for evaluating text-to-image assistants.

Model name	Size	Model Family	Paper
SD-v1-5	400M	U-Net	Rombach et al. (2022)
SDXL	6.6B		Podell et al. (2024)
SDXL Turbo	3.5B		Liu et al. (2024)
Kandinsky 3	12B		Arkhipkin et al. (2023)
Playground-v2-aesthetic	2.6B		Li et al. (2023)
Openjourney	123M		Prompthero (2023)
IF	4.3B	Diffusion Transformers	DeepFloyd.Lab (2023)
SD3	2B		Esser et al. (2024)
PixArt-Sigma	900M		Chen et al. (2024b)
Hunyuan-DiT	1.5B		Li et al. (2024)
FLUX	12B		BlackForestLabs (2024)
Wikimedia Commons[1]	-	Retrieval	Ferrada et al. (2018) Jones & Oyen (2022)

Table 1: List of the approaches evaluated in the Taxonomy Image Generation benchmark.

4 Evaluation

In this section, we describe the evaluation process and metrics.

Our evaluation consists of 9 metrics that we assess to provide a comprehensive evaluation using the latest methods. To formally define our metrics, let V be a finite set of concepts v, $A(v) \subseteq V$ the set of hypernyms for v, and $N(v) \subseteq V$ the set of cohyponyms for v. Let X^j be the set of all possible images x^j in a finite model space $j \in J$ and $|J| = 12$ in our case. We define a mapping $g^j : V \to X^j$ for each model j, which assigns an image to each concept v.

4.1 Preferences Metrics

ELO Scores We evaluate the ELO scores of the model by first assigning pairwise preferences, similar to the modern evaluation of text models Chiang et al. (2024a). Each object v is assigned two uniformly sampled random models $A, B \sim \mathbb{U}[J]$, and their outputs (x^A, x^B) engage in a battle. Then, either a human assessor or GPT-4 serves as a function to assign a win to model A (0) or model

Metric	Mean	Ground Truth				Predicted			
		Easy	Hypo	Hyper	Mix	P-Easy	P-Hypo	P-Hyper	P-Mix
ELO GPT (w/ def)	Playground	Playground	Playground	Playground	Playground	PixArt	PixArt	Playground	SD3[*]
ELO GPT (w/o def)	Playground	Kandinsky3	PixArt[*]	Playground	FLUX	FLUX	Playground	Playground	Kandinsky
ELO Human (w def)	FLUX	Playground / DeepFloyd	Kandinsky3	FLUX	Playground	FLUX	FLUX	Playground	PixArt
ELO Human (w/o def)	FLUX	SD3	Kandinsky3	Playground	PixArt	FLUX	FLUX	SDXL	SDXL
Reward Model (w/ def)	Playground	Playground	Playground	Playground	Playground	Playground	Playground	Playground	Playground
Reward Model (w/o def)	Playground	Playground	Playground	Playground	Playground	Playground	Playground	Playground	Playground
Lemma Similarity	SDXL-turbo	SDXL-turbo	SDXL-turbo	SDXL-turbo	SDXL-turbo	SDXL-turbo	SDXL-turbo	SDXL-turbo	SDXL-turbo
Hypernym Similarity	SDXL-turbo	FLUX	FLUX / SDXL-turbo	SDXL-turbo	FLUX / SDXL-turbo	SDXL-turbo	SDXL-turbo	Draw	Draw
Cohyponyms Similarity	SDXL-turbo	FLUX	SDXL-turbo	SDXL-turbo	SDXL-turbo	SDXL-turbo	SDXL-turbo	SDXL-turbo	SDXL-turbo / SDXL
Specificity	SD1.5	SD1.5 / Playground	SD1.5	SD1.5 / Playground	Draw	Draw	SDXL-turbo / SDXL	SDXL-turbo	SDXL-turbo
FID	SD1.5	FLUX	FLUX	FLUX	HDiT	FLUX	FLUX	FLUX	DeepFloyd
IS	SD3	PixArt	Playground	Playground	SD3	SD3	FLUX	FLUX / Retrieval	Playground

Table 2: Summary of the Top-1 model for each metric and subset. Each cell shows the best-rated model. If two models tie, both are listed with a slash; if more than two tie, ”Draw” is written, indicating insufficient specificity. Results marked with * have negligible differences within the confidence interval. Subsets and models are described in Sections 2 and 3.

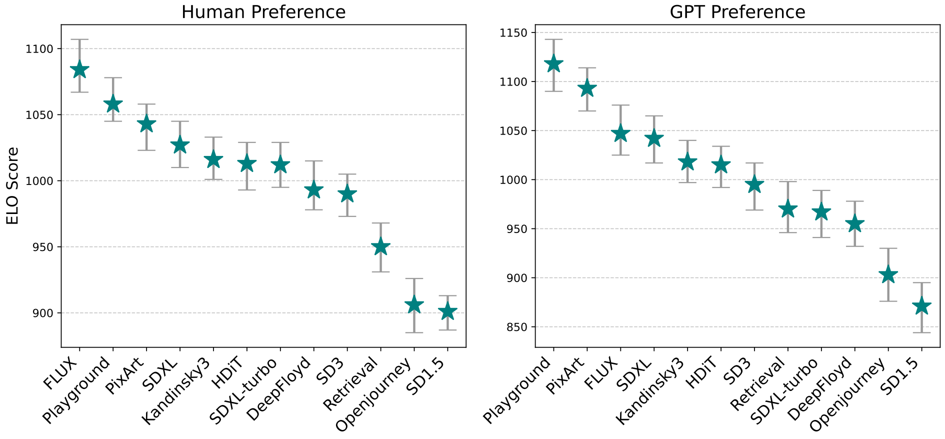

Figure 4: ELO scores for human and GPT4 preferences. The prompt includes the definition. Overall Spearman correlation of model rankings remains significantly high at 0.92, p-value ≤ 0.05.

B (1), represented as $f(v, x^A, x^B) \in \{0, 1\}$. Ties are omitted in both the notation and the BT model. To compute ELO scores, the likelihood is maximized with respect to the BT coefficients for each model, which correspond to their ELO scores. More details of the approach can be found in the Chatbot Arena paper Chiang et al. (2024a).

Following this methodology, we calculate the ELO score based on the Bradley-Terry (BT) model with bootstrapping to build 95% confidence intervals. The Bradley-Terry model Bradley & Terry (1952) is a probabilistic framework used to predict the outcome of pairwise comparisons between items or entities. It assigns a latent strength parameter π to each item i and the probability that item i is preferred over item j is given by: $P(i > j) = \frac{\pi_i}{\pi_i + \pi_j}$. Here, $\pi_i, \pi_j > 0$ represent the strengths of items i and j, respectively. The parameters are typically estimated from observed comparison data using maximum likelihood estimation. We also adopt a labeling technique that includes the “Tie” and “Both Bad” categories, indicating cases where the models are equally good or both produce poor outputs. We modify the prompt from previous studies evaluating text assistants Zheng et al. (2023a) for images, as presented in Figure 3 (also see prompt 7 in Appendix E for more details).

GPT-4 is only one of the nine metrics we report, and it is used as a single comparative signal, not as the core evaluation mechanism. Therefore, we also conduct the **Human ELO Evaluation** along with the **GPT-4 ELO Evaluation** on 3370 pair images from two different models ($\approx$ 600 samples from each model). For Human ELO, we employ 4 assessors expert in computational linguistics, both male and female with at least bachelor degrees. The Spearman correlation between annotators is 0.8 (p-value $\leq$ 0.05) for the images generated with definitions. For the automatic calculation of the ELO score we use GPT-4, which is highly correlated with human evaluations Zheng et al. (2023a) and has proven to be an effective image evaluator on its own Cui et al. (2024), as well as a great pairwise preferences evaluator Chen et al. (2024a).

Reward Model We utilize the reward model from a recent study Xu et al. (2024), which is trained to align with human feedback preferences, focusing on text-image alignment and image fidelity.

This score demonstrates a strong correlation with human annotations and outperformed the CLIP Score and BLIP Score. Formally, this metric is similar to ELO Scores, as the reward model was tuned using preferences and the BT model. However, the key difference is that each object v is assigned a real-valued score and takes only one model image x^j as input: $f_{reward}(v, x^j) \in \mathbb{R}$.

4.2 Similarities

In this section, we introduce novel similarity metrics that leverage taxonomy structure and are derived from KL Divergence and Mutual Information, with formal probabilistic definitions provided in Appendix D. They all have CLIP similarities under the hood, which have been already validated against human judgements Hessel et al. (2021). This ensures that our metrics, by extension, are aligned with human judgements.

In practice, we approximate the probabilities using CLIP similarity Hessel et al. (2021), as it is the most reliable measure of text-image co-occurrence.

Formally, CLIP model $C(\text{text or image}) \in \mathbb{R}^{hidden\_dim}$, we calculate the cosine similarity between the embedding of concept v and the embedding of image x^j, resulting in the score $\text{sim}(C(v), C(x^j))$

Lemma Similarity reflects how well the image aligns with the lemma's textual description; is defined as

$$S_{\text{lemma}}(v,x) := P(X=x|v) \approx \text{sim}(C(v), C(x^j)). \tag{1}$$

Hypernym Similarity reflects how similar the image is on average to the lemma hypernyms; is defined as

$$S_{\text{hyper}}(v,x) := P(X=x|A(v)) = \tfrac{1}{|A(v)|} \textstyle\sum_{a \in A(v)} P(X=x|a) \approx \tfrac{1}{|A(v)|} \displaystyle\sum_{a \in A(v)} \text{sim}(C(a), C(x)). \tag{2}$$

Cohyponym Similarity measures how similar the image is, on average, to the cohyponyms; is defined as

$$S_{\text{cohyponym}}(v,x) := P(X=x|N(v)) = \tfrac{1}{|N(v)|} \textstyle\sum_{n \in N(v)} P(X=x|n) \approx \tfrac{1}{|N(v)|} \displaystyle\sum_{n \in N(v)} \text{sim}(C(n), C(x)). \tag{3}$$

This metric should be interpreted in conjunction with Specificity, as a high Cohyponym Score paired with low Specificity does not necessarily indicate good generation.

In the T2I domain, it is not feasible to define "accuracy" in the traditional sense. It is difficult to determine whether the reflection of a concept is entirely correct or completely incorrect. This challenge is inherent to the nature of T2I tasks and is shared by other studies in this domain. To address this limitation, we propose an analogous measure to assess how well the image reflects the concept. We use the probability of the concept with respect to the generated image, denoted as $P(X = x|v)$, which is derived from Lemma Similarity. To further refine this measure, we also consider how well the generated image fits into the surrounding conceptual space by evaluating Hypernym Similarity and Cohyponym Similarity. These additional metrics help capture how accurately the image represents the broader context of the concept.

In order to understand how well hypernym and co-hyponym similarities correlate with human semantic understanding, we calculated Spearman correlation of the model ranks assigned by these metrics and ranks assigned through the human evaluation ($\rho \approx 0.911, p \leq 0.00004$ for Hypernym CLIP-Score, $\rho \approx 0.871, p \leq 0.00022$ for Co-hyponym CLIP-Score). This demonstrates that the proposed metrics capture relations that humans reliably recognize. Additionally, we would like to specify that WordNet is a human-curated taxonomic structure, which already embeds expert semantic judgments about hypernymy, hyponymy, and siblinghood. WordNet is itself the product of extensive manual linguistic annotation, and therefore provides a reliable human-grounded semantic foundation. Therefore, our evaluation benchmark already assesses how well models connect these human-defined concepts to visual evidence.

Specificity helps to ensure that the image accurately represents the lemma rather than its cohyponyms with the relation of the CLIP-Score to the Cohyponym CLIP-Score $\frac{S_{\text{hyper}}(v,x)}{S_{\text{cohyponym}}(v,x)}$

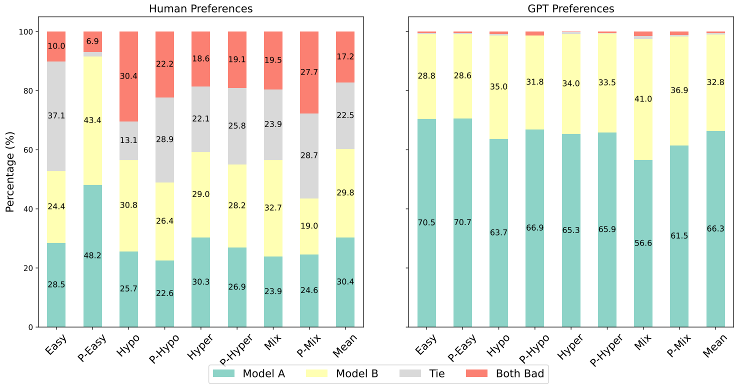

Figure 5: Distribution of preferences for Human and GPT across subsets in percentage (with definition).

This metric generalizes the In-Subtree Probability, as proposed in Baryshnikov & Ryabinin (2023). The key advantage of our metric is that it does not depend on a specific ImageNet classifier and can be applied to any type of taxonomy node.

4.3 FID and IS

We evaluate the Inception Score (IS) Salimans et al. (2016) and the Fréchet Inception Distance (FID) Heusel et al. (2017). IS is primarily used to assess diversity, while FID measures image quality relative to true image distributions. In our case, we calculate FID based on retrieved images, meaning that in this specific setting, FID reflects the "realness" or closeness to retrieval rather than the semantic correctness of an image.

5 Results & Analysis

The summary of the main results are presented in Table 2 and in Appendix H: they show the best model for each subset and each metric. Additionally, we provide an error analysis in Appendix I and discuss the strengths and weaknesses of the best-performing models.

ELO Scores The preferences of human evaluators and GPT-4 resulted in the ELO Scores are shown in Figure 4. FLUX and Playground rank the first and the second across both GPT-4 and human assessors, with PixArt securing the third place. While the other rankings are less consistent—likely due to the difficulty in distinguishing between middle-performing models—the overall Spearman correlation of model rankings remains significantly high at 0.88, p-value ≤ 0.05.

Ranking without definitions is presented in Figure 8 in Appendix G, where FLUX ranks first for the Human preferences and Playground for the GPT Preference. However, the confidence intervals for the GPT Preference suggest it is not a definitive winner, as it ranks similarly to PixArt. The correlation between human and GPT-4 rankings is 0.73, $p \leq 0.05$, which, while lower, is still strong.

At the same time, we found no correlation between raw scores for individual battles. This issue stems from a strong bias toward the first option, as illustrated in Figure 5 and the Confusion Matrix in Figure 12 in Appendix G, a bias not exhibited by humans. Most TTI models benefit from definitions in their input which exposes high human-GPT alignment, as shown in Figure 6 in Appendix C.

Reward Model The results from the Reward Model, introduced in a previous study Xu et al. (2024), show that Playground is the most preferred model, followed by PixArt and FLUX, with no significant differences between the latter, as shown in Figure 10 in Appendix G. Overall, the Reward Model demonstrates a high correlation with human evaluations (0.79) and a moderate correlation with GPT-4 (0.59). Playground is also the preferred model across all subsets, as illustrated in Figure 11 in Appendix G, while Figure 16 in Appendix H highlighting the statistical significance of these comparisons.

Similarities for lemmas, hypernyms, and cohyponyms consistently shows the dominance of SDXL-turbo across all subsets and FLUX for Easy Ground Truth subset. This result differs from AI preferences, possibly due to CLIP-Score focusing solely on text-image alignment without accounting for image quality. It is also noteworthy that SDXL-turbo ranks higher than SDXL, despite being a distilled version of the latter. The distillation process may have preserved more of the image-text alignment features while reducing overall image quality, as suggested in the original paper, while other models are not distilled or are specifically tuned to match user preferences.

Specificity shows no clear dominance, although the top models are SDXL-turbo, SD1.5, and Playground. SD1.5 ranks first in several subsets, though it performs poorly in terms of user preferences. Moreover, this result indicates that Playground's generations can be specific to the precise lemma, aligning both with preference and specificity.

FID results, presented in Table 8 and Table 10 in Appendix H, demonstrate that on average SD1.5 performs best, however FLUX dominates across nearly all subsets. We associate this performance with a stronger focus on reconstructing open-source crawled images, rather than aligning with human preferences and text-image alignment, however FLUX balancing to also appeal to human judgments.

IS results in Table 8 and Table 9 in Appendix H indicate that SD3, Playground, and Retrieval rank first across different subsets, suggesting their generations are perceived as "sharper" and more "distinct". All versions of SDXL and SD3 do not benefit from the definitions, likely due to the specific characteristics of the SD family.

Overall Our results show that Playground and FLUX are among the top models across different metrics, both with and without definitions. While PixArt also demonstrates strong results, it is preferred by AI evaluations more than human preferences, indicating that the preference may be more AI-Judge specific. However, the results are more heterogeneous for specificity, which measures how well the model reflects the concept itself and not its neighbors. Models from the SD family perform differently on different metrics and subsets, indicating that even when models trained with CLIP alignment may not guarantee specificity to the precise concept and the ability to reflect more detailed information of the node.

6 Related Work

In this section, we describe existing evaluation benchmarks for both texts and images and provide an overview of text-to-image generation models. We do not provide an overview on the existing taxonomy-related tasks and approaches and refer to Zeng et al. (2024) and Moskvoretskii et al. (2024b).

Evaluation Benchmarks Popular benchmarks for language models include GLUE Wang et al. (2019) and SuperGLUE Sarlin et al. (2020), MTEB Muennighoff et al. (2023), SQuAD Rajpurkar et al. (2016), MT-Bench Zheng et al. (2023c) and others. For Text2Image Generation, there are benchmarks such as MS-COCO Lin et al. (2014), Fashion-Gen Rostamzadeh et al. (2018) or ConceptBed Patel et al. (2024b). There are also platforms for interactive comparison of AI models, based on ELO-rating: LMSYS Chatbot Arena Chiang et al. (2024b) for LLM and GenAI Arena Jiang et al. (2024a) for comparing text-to-image models. Moreover, due to latest AI's abilities, "LLM-as-a-judge" evaluation emerged: text or image generation outputs of different models are compared by another model, see Zheng et al. (2023c); Wei et al. (2024); Chen et al. (2024a).

Text-to-Image Generation Models For Taxonomies Image generation has recently received significant attention in the field of machine learning. Previously, Generative Adversarial Networks (GANs) (Goodfellow et al., 2014) and Variational Autoencoders (VAEs) (Kingma & Welling, 2014) were primarily used for this purpose. However, diffusion-based methods have now become the dominant approach and are widely used for the visualizations Ng et al. (2024); Sha et al. (2023), but only occasionally for taxonomies Patel et al. (2024a).

To the best of our knowledge, the existing work on the evaluation of images for taxonomies comprises the paper of Baryshnikov & Ryabinin (2023), which introduces In-Subtree Probability (ISP) and Subtree Coverage Score (SCS), which are revisited in our paper. Recently, Liao et al. (2024) introduced a novel task of text-to-image generation for abstract concepts. The benchmark from Patel et al. (2024a) addresses grounded quantitative evaluations of text conditioned concept learners and the Zhang et al. (2024) also operates the notion of concepts for images when developping the concept forgetting and correction method.

7 Conclusion

We have proposed the Taxonomy Image Generation benchmark as a tool for the further evaluation of text-to-image models in taxonomies, as well as for generating images in existing and potentially automatically enriched taxonomies. It consists of 9 metrics and evaluates the ability of 12 open-source text-to-image models to generate images for taxonomy concepts. Our evaluation results show that Playground Li et al. (2023) ranks first in all preference-based evaluations.

Ethical Considerations

In our benchmark, we utilized several text-to-image models as well as text assistants for evaluating and generating new concepts. While these models are highly effective for creating creative and novel content, both textual and visual, they may exhibit various forms of bias. The models tested in this benchmark have the potential to generate malicious or offensive content. However, we are not the creators of these models and focus solely on evaluating their capabilities; therefore, the responsibility for any unfair or malicious usage lies with the users and the models' authors.

Additionally, our fine-tuning of the LLaMA 3.1 model was conducted using safe prompts sourced from WordNet. Although applying quantization and further fine-tuning could potentially reduce the model's safety, we did not observe any unsafe or offensive behavior during our testing.

Reproducibility Considerations

We publish all datasets, generated wordnet images and collected preferences in an anonymous repo.

References

Vladimir Arkhipkin, Andrei Filatov, Viacheslav Vasilev, Anastasia Maltseva, Said Azizov, Igor Pavlov, Julia Agafonova, Andrey Kuznetsov, and Denis Dimitrov. Kandinsky 3.0 technical report. *arXiv preprint arXiv:2312.03511*, 2023.

Anton Baryshnikov and Max Ryabinin. Hypernymy understanding evaluation of text-to-image models via wordnet hierarchy. *arXiv preprint arXiv:2310.09247*, 2023.

BlackForestLabs. Announcements, 2024. URL https://blackforestlabs.ai/announcements/.

Ralph Allan Bradley and Milton E Terry. Rank analysis of incomplete block designs: I. the method of paired comparisons. *Biometrika*, 39(3/4):324–345, 1952. doi: 10.1093/biomet/39.3-4.324.

Dongping Chen, Ruoxi Chen, Shilin Zhang, Yaochen Wang, Yinuo Liu, Huichi Zhou, Qihui Zhang, Yao Wan, Pan Zhou, and Lichao Sun. Mllm-as-a-judge: Assessing multimodal llm-as-a-judge with vision-language benchmark. In *Forty-first International Conference on Machine Learning, ICML 2024, Vienna, Austria, July 21-27, 2024*. OpenReview.net, 2024a. URL https://openreview.net/forum?id=dbFEFHAD79.

Junsong Chen, Chongjian Ge, Enze Xie, Yue Wu, Lewei Yao, Xiaozhe Ren, Zhongdao Wang, Ping Luo, Huchuan Lu, and Zhenguo Li. Pixart-Σ: Weak-to-strong training of diffusion transformer for 4k text-to-image generation. In Ales Leonardis, Elisa Ricci, Stefan Roth, Olga Russakovsky, Torsten Sattler, and Gül Varol (eds.), *Computer Vision - ECCV 2024 - 18th European Conference, Milan, Italy, September 29-October 4, 2024, Proceedings, Part XXXII*, volume 15090 of *Lecture Notes in Computer Science*, pp. 74–91. Springer, 2024b. doi: 10.1007/978-3-031-73411-3_5. URL https://doi.org/10.1007/978-3-031-73411-3_5.

Wei-Lin Chiang, Lianmin Zheng, Ying Sheng, Anastasios Nikolas Angelopoulos, Tianle Li, Dacheng Li, Hao Zhang, Banghua Zhu, Michael Jordan, Joseph E. Gonzalez, and Ion Stoica. Chatbot arena: An open platform for evaluating llms by human preference, 2024a. URL https://arxiv.org/abs/2403.04132.

Wei-Lin Chiang, Lianmin Zheng, Ying Sheng, Anastasios Nikolas Angelopoulos, Tianle Li, Dacheng Li, Banghua Zhu, Hao Zhang, Michael I. Jordan, Joseph E. Gonzalez, and Ion Stoica. Chatbot arena: An open platform for evaluating llms by human preference. In *Forty-first International Conference on Machine Learning, ICML 2024, Vienna, Austria, July 21-27, 2024*. OpenReview.net, 2024b. URL https://openreview.net/forum?id=3MW8GKNyzI.

Xiao Cui, Qi Sun, Wengang Zhou, and Houqiang Li. Exploring GPT-4 vision for text-to-image synthesis evaluation. In *The Second Tiny Papers Track at ICLR 2024*, 2024. URL https://openreview.net/forum?id=xmQoodG82a.

DeepFloyd.Lab. Deepfloyd if, 2023. URL https://github.com/deep-floyd/IF.

Jia Deng, Wei Dong, Richard Socher, Li-Jia Li, Kai Li, and Li Fei-Fei. Imagenet: A large-scale hierarchical image database. In *2009 IEEE conference on computer vision and pattern recognition*, pp. 248–255. Ieee, 2009.

Yilun Du, Sherry Yang, Bo Dai, Hanjun Dai, Ofir Nachum, Josh Tenenbaum, Dale Schuurmans, and Pieter Abbeel. Learning universal policies via text-guided video generation. In A. Oh, T. Naumann, A. Globerson, K. Saenko, M. Hardt, and S. Levine (eds.), *Advances in Neural Information Processing Systems*, volume 36, pp. 9156–9172. Curran Associates, Inc., 2023. URL https://proceedings.neurips.cc/paper_files/paper/2023/file/1d5b9233ad716a43be5c0d3023cb82d0-Paper-Conference.pdf.

Abhimanyu Dubey, Abhinav Jauhri, Abhinav Pandey, Abhishek Kadian, Ahmad Al-Dahle, Aiesha Letman, Akhil Mathur, Alan Schelten, Amy Yang, Angela Fan, Anirudh Goyal, Anthony Hartshorn, Aobo Yang, Archi Mitra, Archie Sravankumar, Artem Korenev, Arthur Hinsvark, Arun Rao, Aston Zhang, Aurélien Rodriguez, Austen Gregerson, Ava Spataru, Baptiste Rozière, Bethany Biron, Binh Tang, Bobbie Chern, and et al. The llama 3 herd of models. *CoRR*, abs/2407.21783, 2024. doi: 10.48550/ARXIV.2407.21783. URL https://doi.org/10.48550/arXiv.2407.21783.

Reza Esfandiarpoor and Stephen H Bach. Follow-up differential descriptions: Language models resolve ambiguities for image classification. *arXiv preprint arXiv:2311.07593*, 2023.

Reza Esfandiarpoor, Cristina Menghini, and Stephen H Bach. If clip could talk: Understanding vision-language model representations through their preferred concept descriptions. *arXiv preprint arXiv:2403.16442*, 2024.

Patrick Esser, Sumith Kulal, Andreas Blattmann, Rahim Entezari, Jonas Müller, Harry Saini, Yam Levi, Dominik Lorenz, Axel Sauer, Frederic Boesel, Dustin Podell, Tim Dockhorn, Zion English, and Robin Rombach. Scaling rectified flow transformers for high-resolution image synthesis. In *Forty-first International Conference on Machine Learning, ICML 2024, Vienna, Austria, July 21-27, 2024*. OpenReview.net, 2024. URL https://openreview.net/forum?id=FPnUhsQJ5B.

Mariia Fedorova, Andrey Kutuzov, and Yves Scherrer. Definition generation for lexical semantic change detection. In Lun-Wei Ku, Andre Martins, and Vivek Srikumar (eds.), *Findings of the Association for Computational Linguistics: ACL 2024*, pp. 5712–5724, Bangkok, Thailand, August 2024. Association for Computational Linguistics. doi: 10.18653/v1/2024.findings-acl.339. URL https://aclanthology.org/2024.findings-acl.339.

Sebastián Ferrada, Nicolás Bravo, Benjamin Bustos, and Aidan Hogan. Querying wikimedia images using wikidata facts. In *Companion Proceedings of the The Web Conference 2018*, WWW '18, pp. 1815–1821, Republic and Canton of Geneva, CHE, 2018. International World Wide Web Conferences Steering Committee. ISBN 9781450356404. doi: 10.1145/3184558.3191646. URL https://doi.org/10.1145/3184558.3191646.

Ian J. Goodfellow, Jean Pouget-Abadie, Mehdi Mirza, Bing Xu, David Warde-Farley, Sherjil Ozair, Aaron C. Courville, and Yoshua Bengio. Generative adversarial nets. In Zoubin Ghahramani, Max Welling, Corinna Cortes, Neil D. Lawrence, and Kilian Q. Weinberger (eds.), *Advances in Neural Information Processing Systems 27: Annual Conference on Neural Information Processing Systems 2014, December 8-13 2014, Montreal, Quebec, Canada*, pp. 2672–2680, 2014. URL https://proceedings.neurips.cc/paper/2014/hash/5ca3e9b122f61f8f06494c97b1afccf3-Abstract.html.

Jack Hessel, Ari Holtzman, Maxwell Forbes, Ronan Le Bras, and Yejin Choi. Clipscore: A reference-free evaluation metric for image captioning. *arXiv preprint arXiv:2104.08718*, 2021.

Martin Heusel, Hubert Ramsauer, Thomas Unterthiner, Bernhard Nessler, and Sepp Hochreiter. Gans trained by a two time-scale update rule converge to a local nash equilibrium. *Advances in neural information processing systems*, 30, 2017.

Dongfu Jiang, Max Ku, Tianle Li, Yuansheng Ni, Shizhuo Sun, Rongqi Fan, and Wenhu Chen. Genai arena: An open evaluation platform for generative models, 2024a. URL https://arxiv.org/abs/2406.04485.

Juyong Jiang, Fan Wang, Jiasi Shen, Sungju Kim, and Sunghun Kim. A survey on large language models for code generation, 2024b. URL https://arxiv.org/abs/2406.00515.

Shawn M Jones and Diane Oyen. Abstract images have different levels of retrievability per reverse image search engine. In *European Conference on Computer Vision*, pp. 203–222. Springer, 2022.

Diederik P. Kingma and Max Welling. Auto-encoding variational bayes. In Yoshua Bengio and Yann LeCun (eds.), *2nd International Conference on Learning Representations, ICLR 2014, Banff, AB, Canada, April 14-16, 2014, Conference Track Proceedings*, 2014. URL http://arxiv.org/abs/1312.6114.

Mirko Lenz and Ralph Bergmann. Case-based adaptation of argument graphs with wordnet and large language models. In Stewart Massie and Sutanu Chakraborti (eds.), *Case-Based Reasoning Research and Development*, pp. 263–278, Cham, 2023. Springer Nature Switzerland. ISBN 978-3-031-40177-0.

Daiqing Li, Aleks Kamko, Ali Sabet, Ehsan Akhgari, Linmiao Xu, and Suhail Doshi. Playground v2, 2023. URL https://huggingface.co/playgroundai/playground-v2-1024px-aesthetic.

Zhimin Li, Jianwei Zhang, Qin Lin, Jiangfeng Xiong, Yanxin Long, Xinchi Deng, Yingfang Zhang, Xingchao Liu, Minbin Huang, Zedong Xiao, Dayou Chen, Jiajun He, Jiahao Li, Wenyue Li, Chen Zhang, Rongwei Quan, Jianxiang Lu, Jiabin Huang, Xiaoyan Yuan, Xiaoxiao Zheng, Yixuan Li, Jihong Zhang, Chao Zhang, Meng Chen, Jie Liu, Zheng Fang, Weiyan Wang, Jinbao Xue, Yangyu Tao, Jianchen Zhu, Kai Liu, Sihuan Lin, Yifu Sun, Yun Li, Dongdong Wang, Mingtao Chen, Zhichao Hu, Xiao Xiao, Yan Chen, Yuhong Liu, Wei Liu, Di Wang, Yong Yang, Jie Jiang, and Qinglin Lu. Hunyuan-dit: A powerful multi-resolution diffusion transformer with fine-grained chinese understanding, 2024.

Jiayi Liao, Xu Chen, Qiang Fu, Lun Du, Xiangnan He, Xiang Wang, Shi Han, and Dongmei Zhang. Text-to-image generation for abstract concepts. In Michael J. Wooldridge, Jennifer G. Dy, and Sriraam Natarajan (eds.), *Thirty-Eighth AAAI Conference on Artificial Intelligence, AAAI 2024, Thirty-Sixth Conference on Innovative Applications of Artificial Intelligence, IAAI 2024, Fourteenth Symposium on Educational Advances in Artificial Intelligence, EAAI 2014, February 20-27, 2024, Vancouver, Canada*, pp. 3360–3368. AAAI Press, 2024. doi: 10.1609/AAAI.V38I4.28122. URL https://doi.org/10.1609/aaai.v38i4.28122.

Tsung-Yi Lin, Michael Maire, Serge J. Belongie, James Hays, Pietro Perona, Deva Ramanan, Piotr Dollár, and C. Lawrence Zitnick. Microsoft COCO: common objects in context. In David J. Fleet, Tomás Pajdla, Bernt Schiele, and Tinne Tuytelaars (eds.), *Computer Vision - ECCV 2014 - 13th European Conference, Zurich, Switzerland, September 6-12, 2014, Proceedings, Part V*, volume 8693 of *Lecture Notes in Computer Science*, pp. 740–755. Springer, 2014. doi: 10.1007/978-3-319-10602-1_48. URL https://doi.org/10.1007/978-3-319-10602-1_48.

Bochao Liu, Pengju Wang, and Shiming Ge. Learning differentially private diffusion models via stochastic adversarial distillation. In Ales Leonardis, Elisa Ricci, Stefan Roth, Olga Russakovsky, Torsten Sattler, and Gül Varol (eds.), *Computer Vision - ECCV 2024 - 18th European Conference, Milan, Italy, September 29-October 4, 2024, Proceedings, Part VII*, volume 15065 of *Lecture Notes in Computer Science*, pp. 55–71. Springer, 2024. doi: 10.1007/978-3-031-72667-5_4. URL https://doi.org/10.1007/978-3-031-72667-5_4.

Rui Mao, Chenghua Lin, and Frank Guerin. Word embedding and WordNet based metaphor identification and interpretation. In Iryna Gurevych and Yusuke Miyao (eds.), *Proceedings of the 56th Annual Meeting of the Association for Computational Linguistics (Volume 1: Long Papers)*, pp. 1222–1231, Melbourne, Australia, July 2018. Association for Computational Linguistics. doi: 10.18653/v1/P18-1113. URL https://aclanthology.org/P18-1113.

George A Miller. *WordNet: An electronic lexical database*. MIT press, 1998.

Viktor Moskvoretskii, Ekaterina Neminova, Alina Lobanova, Alexander Panchenko, and Irina Nikishina. Taxollama: Wordnet-based model for solving multiple lexical sematic tasks. *arXiv preprint arXiv:2403.09207*, 2024a.

Viktor Moskvoretskii, Alexander Panchenko, and Irina Nikishina. Are large language models good at lexical semantics? a case of taxonomy learning. In Nicoletta Calzolari, Min-Yen Kan, Veronique Hoste, Alessandro Lenci, Sakriani Sakti, and Nianwen Xue (eds.), *Proceedings of the 2024 Joint International Conference on Computational Linguistics, Language Resources and Evaluation (LREC-COLING 2024)*, pp. 1498–1510, Torino, Italia, May 2024b. ELRA and ICCL. URL https://aclanthology.org/2024.lrec-main.133.

Niklas Muennighoff, Nouamane Tazi, Loic Magne, and Nils Reimers. MTEB: Massive text embedding benchmark. In Andreas Vlachos and Isabelle Augenstein (eds.), *Proceedings of the 17th Conference of the European Chapter of the Association for Computational Linguistics*, pp. 2014–2037, Dubrovnik, Croatia, May 2023. Association for Computational Linguistics. doi: 10.18653/v1/2023.eacl-main.148. URL https://aclanthology.org/2023.eacl-main.148.

Kam Woh Ng, Xiatian Zhu, Yi-Zhe Song, and Tao Xiang. Partcraft: Crafting creative objects by parts. In Ales Leonardis, Elisa Ricci, Stefan Roth, Olga Russakovsky, Torsten Sattler, and Gül Varol (eds.), *Computer Vision - ECCV 2024 - 18th European Conference, Milan, Italy, September 29-October 4, 2024, Proceedings, Part IX*, volume 15067 of *Lecture Notes in Computer Science*, pp. 420–437. Springer, 2024. doi: 10.1007/978-3-031-72673-6_23. URL https://doi.org/10.1007/978-3-031-72673-6_23.

Irina Nikishina, Polina Chernomorchenko, Anastasiia Demidova, Alexander Panchenko, and Chris Biemann. Predicting terms in is-a relations with pre-trained transformers. In *Findings of the Association for Computational Linguistics: IJCNLP-AACL 2023 (Findings)*, pp. 134–148, 2023.

Maitreya Patel, Tejas Gokhale, Chitta Baral, and Yezhou Yang. Conceptbed: Evaluating concept learning abilities of text-to-image diffusion models. In *AAAI*, pp. 14554–14562. AAAI Press, 2024a.

Maitreya Patel, Tejas Gokhale, Chitta Baral, and Yezhou Yang. Conceptbed: Evaluating concept learning abilities of text-to-image diffusion models. In Michael J. Wooldridge, Jennifer G. Dy, and Sriraam Natarajan (eds.), *Thirty-Eighth AAAI Conference on Artificial Intelligence, AAAI 2024, Thirty-Sixth Conference on Innovative Applications of Artificial Intelligence, IAAI 2024, Fourteenth Symposium on Educational Advances in Artificial Intelligence, EAAI 2014, February 20-27, 2024, Vancouver, Canada*, pp. 14554–14562. AAAI Press, 2024b. doi: 10.1609/AAAI.V38I13.29371. URL https://doi.org/10.1609/aaai.v38i13.29371.

Dustin Podell, Zion English, Kyle Lacey, Andreas Blattmann, Tim Dockhorn, Jonas Müller, Joe Penna, and Robin Rombach. SDXL: improving latent diffusion models for high-resolution image synthesis. In *The Twelfth International Conference on Learning Representations, ICLR 2024, Vienna, Austria, May 7-11, 2024*. OpenReview.net, 2024. URL https://openreview.net/forum?id=di52zR8xgf.

Prompthero. Openjourney, 2023. URL https://huggingface.co/prompthero/openjourney.

Alec Radford, Jong Wook Kim, Chris Hallacy, Aditya Ramesh, Gabriel Goh, Sandhini Agarwal, Girish Sastry, Amanda Askell, Pamela Mishkin, Jack Clark, Gretchen Krueger, and Ilya Sutskever. Learning transferable visual models from natural language supervision. In Marina Meila and Tong Zhang (eds.), *Proceedings of the 38th International Conference on Machine Learning, ICML 2021, 18-24 July 2021, Virtual Event*, volume 139 of *Proceedings of Machine Learning Research*, pp. 8748–8763. PMLR, 2021. URL http://proceedings.mlr.press/v139/radford21a.html.

Colin Raffel, Noam Shazeer, Adam Roberts, Katherine Lee, Sharan Narang, Michael Matena, Yanqi Zhou, Wei Li, and Peter J. Liu. Exploring the limits of transfer learning with a unified text-to-text transformer. *J. Mach. Learn. Res.*, 21:140:1–140:67, 2020. URL https://jmlr.org/papers/v21/20-074.html.

Pranav Rajpurkar, Jian Zhang, Konstantin Lopyrev, and Percy Liang. Squad: 100, 000+ questions for machine comprehension of text. In Jian Su, Xavier Carreras, and Kevin Duh (eds.), *Proceedings of the 2016 Conference on Empirical Methods in Natural Language Processing, EMNLP 2016, Austin, Texas, USA, November 1-4, 2016*, pp. 2383–2392. The Association for Computational Linguistics, 2016. doi: 10.18653/V1/D16-1264. URL https://doi.org/10.18653/v1/d16-1264.

Robin Rombach, Andreas Blattmann, Dominik Lorenz, Patrick Esser, and Björn Ommer. High-resolution image synthesis with latent diffusion models. In *Proceedings of the IEEE/CVF Conference on Computer Vision and Pattern Recognition (CVPR)*, pp. 10684–10695, June 2022.

Negar Rostamzadeh, Seyedarian Hosseini, Thomas Boquet, Wojciech Stokowiec, Ying Zhang, Christian Jauvin, and Chris Pal. Fashion-gen: The generative fashion dataset and challenge, 2018. URL https://arxiv.org/abs/1806.08317.

Tim Salimans, Ian Goodfellow, Wojciech Zaremba, Vicki Cheung, Alec Radford, and Xi Chen. Improved techniques for training gans. *Advances in neural information processing systems*, 29, 2016.

Paul-Edouard Sarlin, Daniel DeTone, Tomasz Malisiewicz, and Andrew Rabinovich. Superglue: Learning feature matching with graph neural networks. In *2020 IEEE/CVF Conference on Computer Vision and Pattern Recognition (CVPR)*, pp. 4937–4946, 2020. doi: 10.1109/CVPR42600.2020.00499.

Zeyang Sha, Zheng Li, Ning Yu, and Yang Zhang. DE-FAKE: detection and attribution of fake images generated by text-to-image generation models. In Weizhi Meng, Christian Damsgaard Jensen, Cas Cremers, and Engin Kirda (eds.), *Proceedings of the 2023 ACM SIGSAC Conference on Computer and Communications Security, CCS 2023, Copenhagen, Denmark, November 26-30, 2023*, pp. 3418–3432. ACM, 2023. doi: 10.1145/3576915.3616588. URL https://doi.org/10.1145/3576915.3616588.

Zhen Tan, Dawei Li, Song Wang, Alimohammad Beigi, Bohan Jiang, Amrita Bhattacharjee, Mansooreh Karami, Jundong Li, Lu Cheng, and Huan Liu. Large language models for data annotation: A survey, 2024. URL https://arxiv.org/abs/2402.13446.

Alex Wang, Amanpreet Singh, Julian Michael, Felix Hill, Omer Levy, and Samuel R. Bowman. GLUE: A multi-task benchmark and analysis platform for natural language understanding. In *7th International Conference on Learning Representations, ICLR 2019, New Orleans, LA, USA, May 6-9, 2019*. OpenReview.net, 2019. URL https://openreview.net/forum?id=rJ4km2R5t7.

Zijie J. Wang, Evan Montoya, David Munechika, Haoyang Yang, Benjamin Hoover, and Duen Horng Chau. DiffusionDB: A large-scale prompt gallery dataset for text-to-image generative models. In Anna Rogers, Jordan Boyd-Graber, and Naoaki Okazaki (eds.), *Proceedings of the 61st Annual Meeting of the Association for Computational Linguistics (Volume 1: Long Papers)*, pp. 893–911, Toronto, Canada, July 2023. Association for Computational Linguistics. doi: 10.18653/v1/2023.acl-long.51. URL `https://aclanthology.org/2023.acl-long.51`.

Hui Wei, Shenghua He, Tian Xia, Andy Wong, Jingyang Lin, and Mei Han. Systematic evaluation of llm-as-a-judge in llm alignment tasks: Explainable metrics and diverse prompt templates, 2024. URL `https://arxiv.org/abs/2408.13006`.

Jiazheng Xu, Xiao Liu, Yuchen Wu, Yuxuan Tong, Qinkai Li, Ming Ding, Jie Tang, and Yuxiao Dong. Imagereward: Learning and evaluating human preferences for text-to-image generation. *Advances in Neural Information Processing Systems*, 36, 2024.

Qingkai Zeng, Yuyang Bai, Zhaoxuan Tan, Zhenyu Wu, Shangbin Feng, and Meng Jiang. Codetaxo: Enhancing taxonomy expansion with limited examples via code language prompts, 2024. URL `https://arxiv.org/abs/2408.09070`.

Gong Zhang, Kai Wang, Xingqian Xu, Zhangyang Wang, and Humphrey Shi. Forget-me-not: Learning to forget in text-to-image diffusion models. In *IEEE/CVF Conference on Computer Vision and Pattern Recognition, CVPR 2024 - Workshops, Seattle, WA, USA, June 17-18, 2024*, pp. 1755–1764. IEEE, 2024. doi: 10.1109/CVPRW63382.2024.00182. URL `https://doi.org/10.1109/CVPRW63382.2024.00182`.

Lianmin Zheng, Wei-Lin Chiang, Ying Sheng, Siyuan Zhuang, Zhanghao Wu, Yonghao Zhuang, Zi Lin, Zhuohan Li, Dacheng Li, Eric Xing, Hao Zhang, Joseph E Gonzalez, and Ion Stoica. Judging llm-as-a-judge with mt-bench and chatbot arena. In A. Oh, T. Naumann, A. Globerson, K. Saenko, M. Hardt, and S. Levine (eds.), *Advances in Neural Information Processing Systems*, volume 36, pp. 46595–46623. Curran Associates, Inc., 2023a. URL `https://proceedings.neurips.cc/paper_files/paper/2023/file/91f18a1287b398d378ef22505bf41832-Paper-Datasets_and_Benchmarks.pdf`.

Lianmin Zheng, Wei-Lin Chiang, Ying Sheng, Siyuan Zhuang, Zhanghao Wu, Yonghao Zhuang, Zi Lin, Zhuohan Li, Dacheng Li, Eric P. Xing, Hao Zhang, Joseph E. Gonzalez, and Ion Stoica. Judging llm-as-a-judge with mt-bench and chatbot arena. In Alice Oh, Tristan Naumann, Amir Globerson, Kate Saenko, Moritz Hardt, and Sergey Levine (eds.), *Advances in Neural Information Processing Systems 36: Annual Conference on Neural Information Processing Systems 2023, NeurIPS 2023, New Orleans, LA, USA, December 10 - 16, 2023*, 2023b. URL `http://papers.nips.cc/paper_files/paper/2023/hash/91f18a1287b398d378ef22505bf41832-Abstract-Datasets_and_Benchmarks.html`.

Lianmin Zheng, Wei-Lin Chiang, Ying Sheng, Siyuan Zhuang, Zhanghao Wu, Yonghao Zhuang, Zi Lin, Zhuohan Li, Dacheng Li, Eric P. Xing, Hao Zhang, Joseph E. Gonzalez, and Ion Stoica. Judging llm-as-a-judge with mt-bench and chatbot arena. In Alice Oh, Tristan Naumann, Amir Globerson, Kate Saenko, Moritz Hardt, and Sergey Levine (eds.), *Advances in Neural Information Processing Systems 36: Annual Conference on Neural Information Processing Systems 2023, NeurIPS 2023, New Orleans, LA, USA, December 10 - 16, 2023*, 2023c. URL `http://papers.nips.cc/paper_files/paper/2023/hash/91f18a1287b398d378ef22505bf41832-Abstract-Datasets_and_Benchmarks.html`.

Chunting Zhou, Pengfei Liu, Puxin Xu, Srini Iyer, Jiao Sun, Yuning Mao, Xuezhe Ma, Avia Efrat, Ping Yu, Lili Yu, Susan Zhang, Gargi Ghosh, Mike Lewis, Luke Zettlemoyer, and Omer Levy. Lima: Less is more for alignment, 2023. URL `https://arxiv.org/abs/2305.11206`.

A LIMITATIONS

- Our evaluation focuses on open-source text-to-image models, as they are more convenient and cost-effective to use in any system than models relying on an API. Additionally, open-source models offer the flexibility for fine-tuning, which is not possible with closed-source models. However, it would be valuable to explore how closed-source models perform on this task, as our benchmark depends solely on the quality of the generated images.
- Preferences using GPT-4 were obtained with the use of Chain of Thought reasoning, following previous studies to optimize the prompt Zheng et al. (2023a). However, we did not utilize multiple generations with a majority vote to improve consistency, nor did we rename the models, which could help reduce positional bias. Additionally, we did not perform multiple runs with models alternating positions, as each model could appear in position A or B with equal probability. The Bradley-Terry model of preferences compensates for such inconsistencies and provides robust scoring, given a sufficient number of preference labels, as noted in a previous study Zheng et al. (2023a). Our assumption is further supported by the high correlation in the resulting rankings, even though the correlation between raw preferences is close to zero.
- Metrics based on CLIP-Score may be biased toward the CLIP model and lack specificity if CLIP is unfamiliar with or unspecific to the precise WordNet concept. Additionally, models could be fine-tuned to optimize for this particular metric. To mitigate this bias, we propose incorporating preferences from AI feedback and also employ preferences from human feedback to provide a more balanced and comprehensive evaluation.
- The Inception Score relies on the InceptionV3 model, which is specific to ImageNet1k. We included this metric as it is traditionally used to measure overall text-to-image performance. However, to address this potential bias, we introduced CLIP based metrics as well as generalization of the ISP metric from a previous study Baryshnikov & Ryabinin (2023), which also relies on an ImageNet1k classifier, but we supplemented it with the use of CLIP to provide a broader evaluation.
- The benchmark focuses mainly on WordNet concepts, which may limit generalization to other (multilingual) taxonomies or domains that differ in structure. Extending the benchmark to other resources (e.g. Wikidata, ConceptNet) would require substantial additional design and alignment work and is therefore a separate research direction. In the present paper, we intentionally focus on WordNet because it provides the clearest foundation for linguistic evaluation of model representations.

B TTI MODELS DESCRIPTION

To generate the images, we employed ten models and one retrieval approach. It results in 12 systems in total.

B.1 U-NET-BASED MODELS

Models based on the architecture:

- **SD-v1-5** (400M) (Rombach et al., 2022) is a SD-v1-2 fine-tuned on 595k steps at resolution 512x512 on “laion-aesthetics v2 5+” and 10% dropping of the text-conditioning to improve classifier-free guidance sampling.
- **SDXL** (6.6B) (Podell et al., 2024). The U-Net within is 3 times larger comparing to classical SD models. Moreover, additional CLIP (Radford et al., 2021) text encoder is utilized increasing the number of parameters.
- **SDXL Turbo** (3.5B) (Liu et al., 2024) is a distilled version of SDXL-1.0.
- **Kandinsky 3** (12B) (Arkhipkin et al., 2023). The sizes of U-Net and text encoders were significantly increased in comparison to the second generation.
- **Playground-v2-aesthetic** (2.6B) (Li et al., 2023) has the same architecture as SDXL, and is trained on a dataset from Midjourney[2].

[2] https://www.midjourney.com

- **Openjourney** (123M) (Prompthero, 2023) is also trained on Midjourney images.

B.2 Diffusion Transformers models

Diffusion Transformers (DiTs) models:

- **IF** (4.3B) (DeepFloyd.Lab, 2023). A modular system consisting of a frozen text encoder and three sequential pixel diffusion modules.
- **SD3** (2B) (Esser et al., 2024) is a Multimodal DiT (MMDiT). The authors used two CLIP encoders and T5 (Raffel et al., 2020) for combining visual and textual inputs.
- **PixArt-Sigma** (900M) (Chen et al., 2024b). The authors employed novel attention mechanism for the sake of efficiency and high-quality training data for 4K images.
- **Hunyuan-DiT** (1.5B) (Li et al., 2024) is a text-to-image diffusion transformer designed for fine-grained understanding of both English and Chinese, using a custom-built transformer structure and text encoder.
- **FLUX** (12B) BlackForestLabs (2024) is a rectified flow Transformer capable of generating images from text descriptions. It is based on a hybrid architecture of multimodal and parallel diffusion transformer blocks.

B.3 Retrieval

We retrieved images from Wikimedia Commons[3], following previous studies Ferrada et al. (2018); Jones & Oyen (2022). For 3370 total items, this process resulted in 1,790 unique images. For 20 concepts (32 dataset entities), no images were found. For 146 lemmas, the search returned images that had already been retrieved, likely due to the similarity of the concepts searched. We use the top-1 output from the main image search engine[4].

C Definitions Analysis

We also analyzed how different models benefit from the inclusion of definitions in the TTI prompt, examining the change in winning battles with definitions (all models are provided with definitions), as depicted in Figure 6. Most models benefit from definitions according to human evaluation, though the trend is milder in GPT-4 evaluations, with preferences for Kandinsky3 and SD1.5 even dropping significantly. Despite the outlier of Kandinsky3, the overall trend between GPT-4 and human evaluations highlights the alignment of GPT-4's judgments with human preferences.

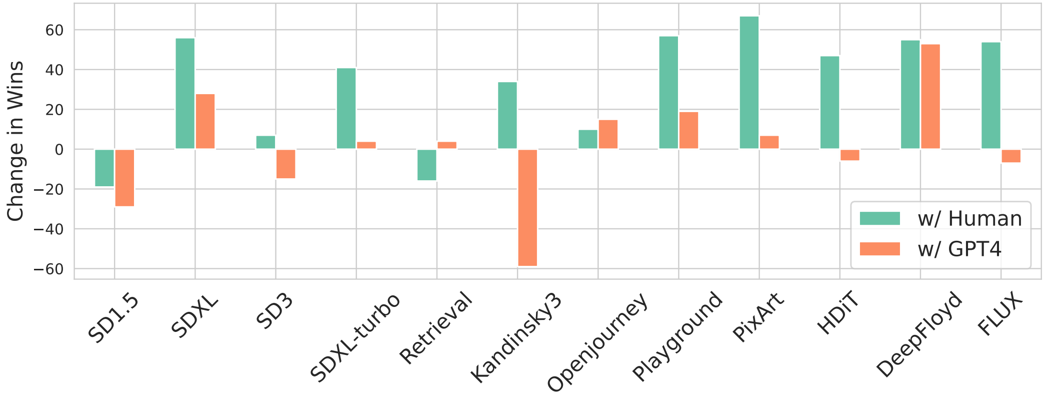

Figure 6: Summary change in battle wins with added definition in prompt.

[3] https://commons.wikimedia.org/

[4] For the lemma "coin", the search URL is https://commons.wikimedia.org/w/index.php?search=coin&title=Special:MediaSearch&go=Go&type=image

D Metrics Definition

Let V be a finite set of concepts (lemmas), where each $v \in V$ represents a semantic category. Let $(\mathcal{X}, \mathcal{A}, \mu)$ be a measurable space representing the image domain, where $\mathcal{X}$ is the set of all possible images, $\mathcal{A}$ is a σ-algebra of measurable subsets of $\mathcal{X}$, and μ is a base measure.

For each concept $v \in V$, we assume a probability measure $P(\cdot \mid v)$ on $(\mathcal{X}, \mathcal{A})$ such that $P(X \in A \mid v)$ represents the probability that an image X generated under the concept v lies in the measurable set A. In other words, each concept v defines a probability distribution over the image space $\mathcal{X}$.

D.1 Lemma Similarity

Definition (Lemma Similarity). *Given a concept $v \in V$ and an image $x \in \mathcal{X}$, the* Lemma Similarity *is defined as:*

$$S_{\textit{lemma}}(v, x) := P(X = x \mid v).$$

This measures the likelihood of observing the image x under the assumption that the concept v is the generating source. According to Theorem 1, it also reflects the likelihood of the concept v given the image x, offering a principled way to assess how well an image aligns with the semantic properties of a concept. Maximizing this metric implies a stronger alignment between the concept and the generated image.

Theorem 1. *Let V be a finite set of concepts, and suppose the prior distribution is uniform $P(V = v) = \frac{1}{|V|}\, \forall v \in V$. Then, $\forall x \in X\, \forall v \in V$ $\arg\max_{i \in V} S_{\textit{lemma}}(v, x) \propto \arg\max_{i \in V} P(V = v \mid X = x)$.*

Proof. By Bayes' rule, the posterior probability of concept i given an image x is:

$$P(V = i \mid X = x) = \frac{P(X = x \mid i)P(V = i)}{\sum_{v \in V} P(X = x \mid v)P(V = v)} = \frac{P(X = x \mid i) \cdot \frac{1}{|V|}}{\sum_{v \in V} P(X = x \mid v) \cdot \frac{1}{|V|}} = \frac{P(X = x \mid i)}{\sum_{v \in V} P(X = x \mid v)} \propto P(X = x \mid i) \tag{4}$$

To find the concept i that maximizes the posterior $P(V = i \mid X = x)$, we write:

$$\hat{i} = \arg\max_{i \in V} P(V = i \mid X = x) = \arg\max_{i \in V} P(X = x \mid i) = \arg\max_{i \in V} S_{\text{lemma}}(i, x).$$

Thus, under a uniform prior, maximizing the posterior probability is equivalent to maximizing the Lemma Similarity □

D.2 Hypernym Similarity & Cohyponym Similarity

Definition (Hypernym Similarity). *Let $A(i) \subseteq V$ be the set of hypernyms of a concept $i \in V$. For a given image $x \in \mathcal{X}$, we define the* Hypernym Similarity *as:*

$$S_{\textit{hyper}}(i, x) := P(X = x \mid A(i)) = \frac{1}{|A(i)|} \sum_{h \in A(i)} P(X = x \mid h).$$

Definition (Cohyponym Similarity). *Let $C(i) \subseteq V$ be the set of cohyponyms of a concept $i \in V$. For a given image $x \in \mathcal{X}$, we define the* Cohyponym Similarity *as:*

$$S_{\textit{cohyponym}}(i, x) := P(X = x \mid C(i)) = \frac{1}{|C(i)|} \sum_{ch \in C(i)} P(X = x \mid ch).$$

Hypernym Similarity and *Cohyponym Similarity* represent the likelihood of observing x under the average distribution of its ancestor and cohyponyms concepts respectively. Intuitively, they measure how well the image x fits into the neighboring concepts either broader, more general semantic category represented by the ancestors of i or similar, slightly different concepts from the same ancestor of i. According further to Theorem 2, maximizing those similarities is proportional to minimizing distance between image space conditioned on a concept and image space conditioned on specific neighbor space, therefore better reflecting neighbors semantic properties and covering tree structure.

Theorem 2. *With large enough $S_{lemma}(i,x)$ to properly represent our concept,* $\max S_{hyper}(i,x)$ *and* $\max S_{cohyponym}(i,x) \propto \min_{P(X|A(i))} D_{KL}\big(P(X \mid i) \,\|\, P(X \mid A(i))\big)$.

Proof. The proof will be based for the ancestor case, however proving for cohyponyms is similar with only change of ancestor set to cohyponyms set.

Consider the KL divergence:

$$D_{\text{KL}}\big(P(X \mid i) \,\|\, P(X \mid A(i))\big) = \sum_{x \in \mathcal{X}} P(X = x \mid i) \log \frac{P(X = x \mid i)}{P(X = x \mid A(i))}.$$

$$\arg \min_{P(X|A(i))} D_{\text{KL}}\big(P(X \mid i) \,\|\, P(X \mid A(i))\big) \implies \frac{P(X = x \mid i)}{P(X = x \mid A(i))} \approx 1 \quad \forall x.$$

As $P(X = x \mid i)$ is fixed in precise setting, achieving $\frac{P(X=x|i)}{P(X=x|A(i))} \approx 1$ requires increasing $P(X = x \mid A(i))$ subject to large enough $P(X = x \mid i)$. Since $S_{\text{hyper}}(i,x) = P(X = x \mid A(i))$, increasing $S_{\text{hyper}}(i,x)$ for the most probable x under i reduces the KL divergence. □

D.3 Specificity

Definition (Specificity)**.** *Let $C(i)$ be the set of cohyponyms of a concept $i \in V$. Define:*

$$P(X = x \mid C(i)) := \frac{1}{|C(i)|} \sum_{c \in C(i)} P(X = x \mid c).$$

The Specificity *of an image $x \in \mathcal{X}$ with respect to a concept $i \in V$ is:*

$$\textit{Spec}(i,x) := \frac{P(X = x \mid i)}{P(X = x \mid C(i))}.$$

Specificity measures how much more likely it is that x was generated by a concept i compared to one of its cohyponyms. A high Specificity value indicates that the probability of x under i is significantly larger than under $C(i)$, the distribution over its cohyponyms. According to Theorems 3 and 4, Specificity highlights the uniqueness of the node representation by maximizing the distance to the cohyponyms nodes distribution and increasing the mutual information between the concept and image spaces. However, this metric relies on a high *Lemma Similarity* value; otherwise, the reflected uniqueness may be misleading due to poor alignment with the target node's distribution.

Theorem 3.

$$\max \textit{Spec}(i,x) \propto \max D_{KL}(P(X \mid i) \| P(X \mid C(i)))$$

Proof.

$$\text{Spec}(i,x) = \frac{P(X = x \mid i)}{P(X = x \mid C(i))}.$$

$$\log(\text{Spec}(i,x)) = \log \frac{P(X = x \mid i)}{P(X = x \mid C(i))}.$$

$$D_{\text{KL}}(P(X \mid i) \| P(X \mid C(i))) = \sum_{x} P(X = x \mid i) \log \frac{P(X = x \mid i)}{P(X = x \mid C(i))}.$$

For fixed $P(X = x \mid i)$, increasing $\frac{P(X=x|i)}{P(X=x|C(i))}$ for all x (i.e., maximizing Spec(i,x)) increases each $\log \frac{P(X=x|i)}{P(X=x|C(i))}$ term. Thus, the sum $D_{\text{KL}}(P(X \mid i) \| P(X \mid C(i)))$ is maximized. □

Theorem 4. *Let V and X be random variables over concepts and images.* $\max \textit{Spec}(i,x) \forall v \in V, x \in X \propto \max I(V;X)$.

Proof.

$$I(V;X) = \sum_{v,x} P(V=v, X=x) \log \frac{P(X=x \mid V=v)}{P(X=x)}.$$

For $v = i$:

$$\frac{P(X=x \mid i)}{P(X=x)} = \frac{P(X=x \mid i)}{\sum_{v'} P(V=v')P(X=x \mid v')}.$$

Consider the uniform prior ($P(V=v') = \frac{1}{|V|}$):

$$P(X=x) = \frac{1}{|V|} \sum_{v'} P(X=x \mid v'), \quad P(X=x \mid C(i)) = \frac{1}{|C(i)|} \sum_{c \in C(i)} P(X=x \mid c).$$

$$\text{Spec}(i,x) = \frac{P(X=x \mid i)}{P(X=x \mid C(i))}.$$

Increasing $\text{Spec}(i,x) \propto \frac{P(X=x|i)}{P(X=x)}$, raising each term $P(V=i, X=x) \log \frac{P(X=x|i)}{P(X=x)}$, thus increasing $I(V;X)$. □

E GPT-4 Prompts

We show the technical style prompt for GPT-4 in Figure 7 for more clarity on how images and user prompt were provided. We employed "gpt-4o-mini" version with API calls with images in high resolution.

The prompt for "gpt-4o-mini" to generate definitions for TaxoLLaMA3.1 predictions is presented below.

(1)

```
Write a definition for the word/phrase in one sentence.

Example:
Word: caddle
Definition: act as a caddie and carry clubs for a player

Word: bichon
Definition:
```

```
Please act as an impartial judge and evaluate the quality of the images provided by two AI
image assistants to the user prompt displayed below.


You should choose the assistant that provides an image that follows the user's instructions
better and reflects the user's prompt main concept better.
Your evaluation should consider factors such as image-text alignment, relevance, accuracy,
depth, and fidelity (overall image quality).
Begin your evaluation by comparing the two images and provide a short explanation.

Avoid any position biases and ensure that the order in which the responses were presented do
not influence your decision.

Do not allow the size of the images to influence your evaluation.
Do not favor certain names of the assistants.
Be as objective as possible.

After providing your explanation, output your final verdict by strictly following this format:

"[[A]]" if assistant A is better, "[[B]]" if assistant B is better, "[[C]]" for a tie and "
[[D]]" if both images are bad.

[User Prompt]

inherited disorder (a genetic condition passed down from parents to their offspring, often
resulting in physical or mental health problems)

[Start of the first image]

<img_a>

[End of the first image]

[Start of the first image]

<img_b>

[End of the first image]
```

Figure 7: Full prompt example for evaluating text-to-image assistants.

F TECHNICAL DETAILS

For text-to-image, we used the recommended generation parameters for each model, the Hugging-Face Diffusers library, and a single NVIDIA A100 GPU. All models were utilized in FP16 precision and produced images with resolutions of 512x512 or 1024x1024. Additionally, we experimented with prompting, adding definitions from the WordNet database to help with ambiguity resolution, as this has shown benefits for LLMs in the past Moskvoretskii et al. (2024b).

G ADDITIONAL FIGURES

In this appendix, we include graphs for our evaluation, which results outlined in the main text.

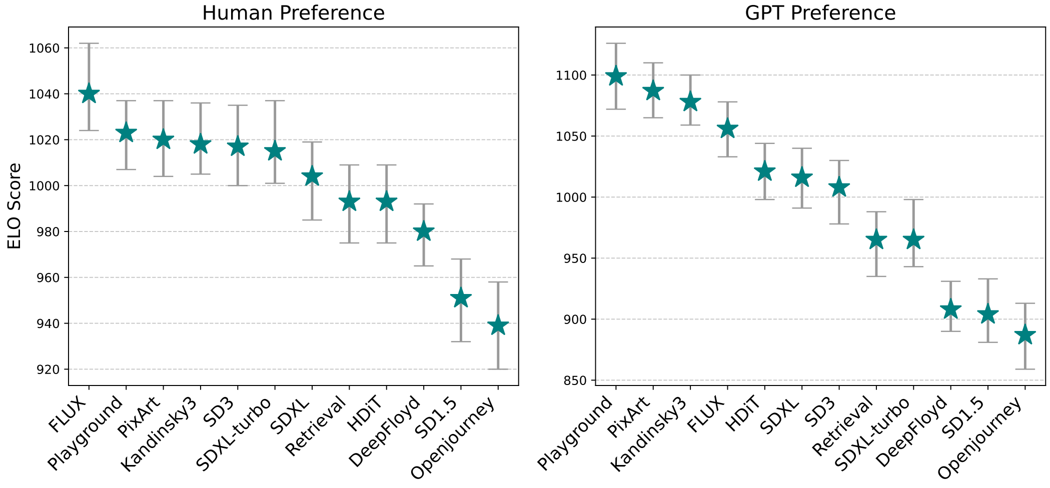

Figure 8: ELO scores for human and GPT4 preferences. Prompt did not include the definition.

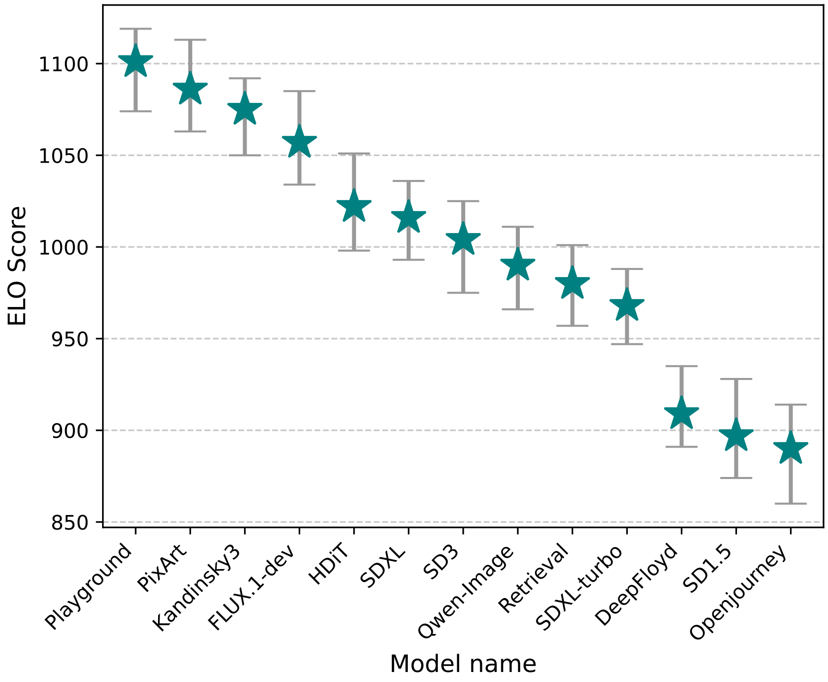

Figure 9: ELO scores for GPT4 preferences with Qwen-Image model. Prompt did not include the definition.

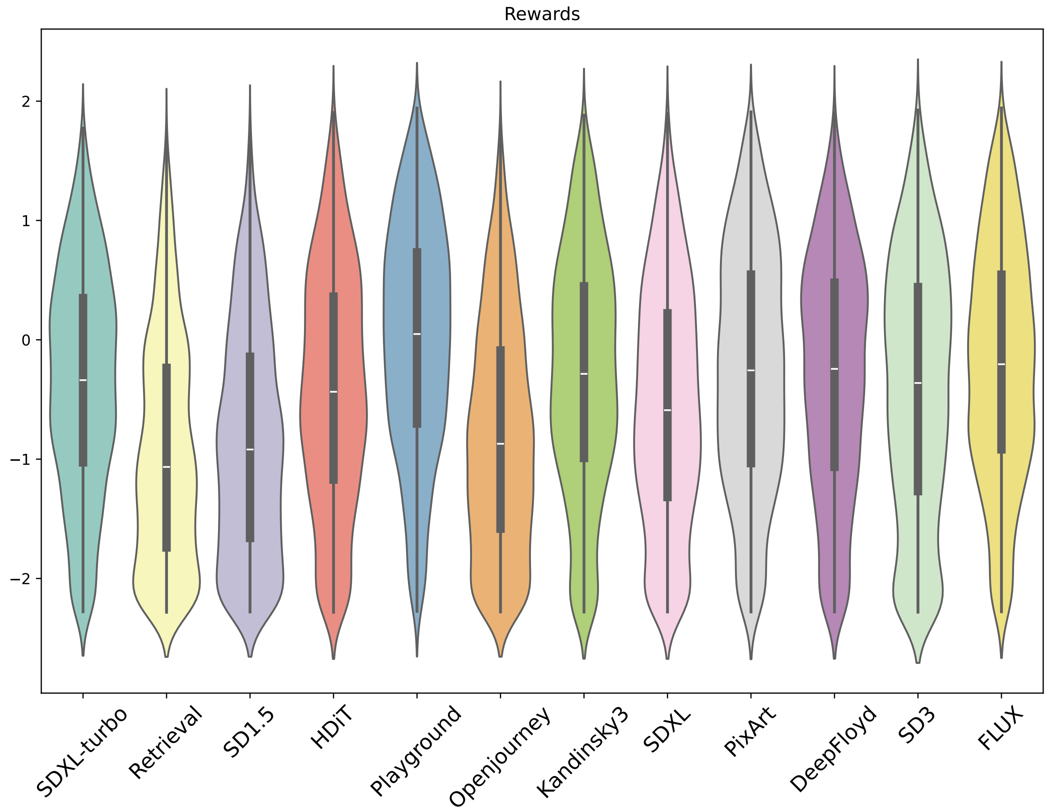

Figure 10: Distribution of rewards for each model, calculated with reward model described in Section 4

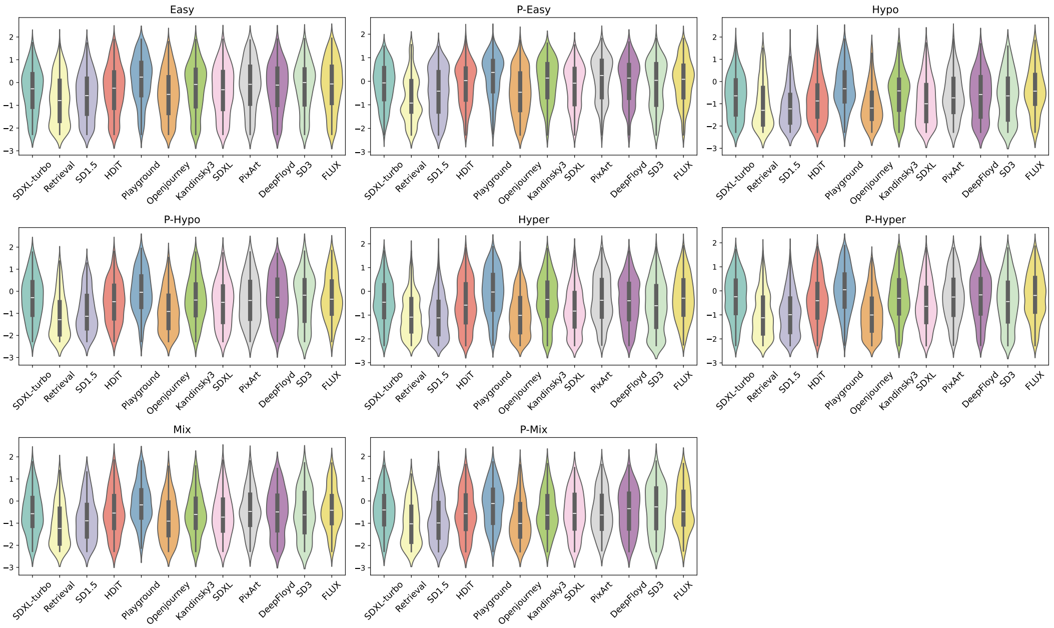

Figure 11: Distribution of rewards for each model across subsets, calculated with reward model described in Section 4

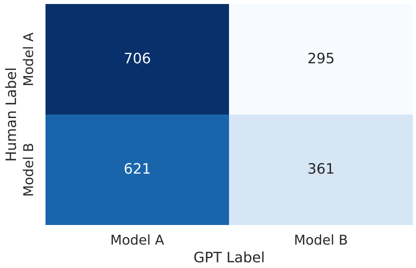

Figure 12: Confusion matrix for human and GPT preferences, excluding Tie labels to avoid distracting the analysis. GPT rarely assigns Ties, with fewer than 20 instances. The prompt included a definition.

Model	Ground Truth				Predicted			
	Easy	Hypo	Hyper	Mix	P-Easy	P-Hypo	P-Hyper	P-Mix
Playground	1125 (+61/-59)	1139 (+137/-111)	1148 (+50/-56)	1066 (+97/-105)	1072 (+87/-85)	1095 (+118/-89)	1141 (+53/-59)	1047 (+130/-105)
FLUX	1013 (+65/-78)	1104 (+153/-151)	1088 (+48/-50)	982 (+105/-125)	1066 (+82/-60)	967 (+131/-107)	1025 (+46/-41)	1096 (+144/-132)
PixArt	1050 (+43/-67)	1125 (+181/-100)	1086 (+60/-40)	1038 (+104/-80)	1135 (+82/-66)	1159 (+143/-95)	1107 (+47/-49)	1063 (+101/-136)
SDXL	960 (+75/-72)	1113 (+145/-149)	1056 (+63/-61)	1063 (+134/-128)	1061 (+78/-67)	1112 (+114/-86)	1050 (+49/-48)	1010 (+148/-120)
HDiT	981 (+61/-61)	955 (+100/-97)	1004 (+44/-51)	1053 (+122/-137)	980 (+78/-59)	1046 (+138/-86)	1074 (+52/-61)	965 (+148/-134)
Kandinsky3	1010 (+72/-70)	1035 (+103/-101)	998 (+51/-55)	958 (+135/-82)	1051 (+74/-55)	999 (+100/-104)	1043 (+48/-40)	1005 (+102/-113)
Retrieval	965 (+81/-76)	884 (+98/-106)	979 (+47/-58)	1014 (+119/-105)	953 (+65/-72)	880 (+111/-135)	995 (+51/-54)	971 (+138/-137)
SD3	1056 (+78/-59)	949 (+118/-99)	962 (+41/-53)	983 (+122/-113)	997 (+49/-59)	1090 (+123/-120)	961 (+62/-57)	1104 (+116/-85)
SDXL-turbo	1004 (+86/-69)	999 (+102/-93)	957 (+49/-48)	960 (+114/-148)	917 (+74/-86)	964 (+82/-117)	969 (+46/-47)	1025 (+110/-102)
DeepFloyd	981 (+53/-63)	909 (+76/-95)	943 (+50/-43)	1053 (+128/-110)	931 (+56/-64)	949 (+152/-158)	941 (+40/-65)	1036 (+105/-109)
Openjourney	997 (+65/-59)	849 (+102/-125)	889 (+56/-62)	962 (+97/-107)	987 (+59/-77)	880 (+87/-162)	826 (+54/-55)	825 (+125/-225)
SD1.5	852 (+69/-90)	933 (+102/-120)	885 (+58/-55)	863 (+110/-115)	842 (+65/-70)	853 (+73/-130)	864 (+48/-64)	847 (+108/-133)

Table 3: ELO score for GPT Preferences for subsets with definition in input.

Model	Ground Truth				Predicted			
	Easy	Hypo	Hyper	Mix	P-Easy	P-Hypo	P-Hyper	P-Mix
Playground	1091 (+82/-47)	1110 (+154/-123)	1116 (+45/-42)	1049 (+159/-101)	1069 (+72/-66)	1136 (+148/-118)	1127 (+66/-53)	1093 (+167/-104)
PixArt	1037 (+77/-71)	1137 (+110/-105)	1113 (+49/-50)	1094 (+103/-90)	1122 (+86/-73)	1048 (+122/-111)	1081 (+45/-46)	1076 (+123/-102)
Kandinsky3	1094 (+66/-74)	1065 (+95/-110)	1090 (+44/-57)	1021 (+84/-107)	1051 (+76/-67)	1083 (+120/-72)	1089 (+46/-52)	1117 (+112/-120)
FLUX	954 (+48/-65)	1030 (+103/-113)	1057 (+55/-57)	1119 (+135/-106)	1137 (+109/-64)	1097 (+122/-100)	1068 (+58/-46)	1032 (+132/-128)
HDiT	1028 (+58/-55)	954 (+102/-129)	1040 (+45/-41)	1039 (+107/-102)	1014 (+92/-56)	1055 (+136/-86)	1028 (+51/-48)	835 (+118/-177)
SDXL	1015 (+52/-61)	939 (+104/-120)	1029 (+58/-50)	998 (+137/-156)	1034 (+63/-64)	998 (+123/-105)	1008 (+44/-45)	1033 (+133/-144)
SD3	1076 (+66/-76)	951 (+108/-103)	1006 (+50/-60)	1099 (+129/-146)	1014 (+62/-65)	969 (+99/-100)	964 (+34/-56)	1078 (+124/-83)
Retrieval	926 (+79/-70)	996 (+99/-110)	973 (+53/-43)	1019 (+127/-109)	917 (+81/-70)	959 (+116/-104)	994 (+49/-45)	938 (+157/-138)
SDXL-turbo	1045 (+76/-56)	969 (+94/-94)	906 (+56/-54)	967 (+104/-150)	950 (+66/-63)	868 (+80/-146)	980 (+43/-45)	1073 (+115/-101)
DeepFloyd	918 (+65/-63)	900 (+131/-90)	903 (+46/-60)	888 (+108/-112)	862 (+56/-86)	976 (+99/-149)	896 (+54/-61)	980 (+125/-125)
SD1.5	870 (+71/-105)	976 (+95/-134)	888 (+58/-49)	925 (+96/-115)	894 (+69/-75)	961 (+90/-80)	905 (+34/-45)	866 (+107/-187)
Openjourney	940 (+76/-50)	969 (+108/-135)	874 (+43/-57)	774 (+93/-139)	930 (+60/-70)	846 (+86/-129)	854 (+47/-60)	872 (+91/-154)

Table 4: ELO score for GPT Preferences for subsets with no definition in input.

H Additional Tables

In this section we provide the detailed tables for every metric evaluated in the paper.

FID results are demonstrated in Tables 8 and 10.

IS results are shown in Tables 9 and 8.

Lemma Similarity results are shown in Table 12

Hypernym Similarity results are shown in Table 11

Cohyponym Similarity results are shown in Table 15

Specificity results are shown in Table 14

Reward model p-values of Mann-Whitney test on comparing means shown in Table 16

ELO Scores for human and GPT labeling within each subset with and without definitions are shown in Tables 3, 4, 5 and 6.

Model	Ground Truth				Predicted			
	Easy	Hypo	Hyper	Mix	P-Easy	P-Hypo	P-Hyper	P-Mix
DeepFloyd	1056 (+45/-38)	957 (+72/-77)	956 (+40/-27)	945 (+89/-85)	1013 (+60/-62)	946 (+64/-90)	993 (+28/-41)	1027 (+55/-60)
Playground	1055 (+37/-46)	1102 (+96/-95)	1078 (+36/-33)	1094 (+81/-64)	1017 (+67/-53)	994 (+63/-62)	1075 (+39/-33)	1019 (+70/-68)
FLUX	1050 (+48/-44)	1105 (+128/-73)	1088 (+37/-38)	1048 (+104/-97)	1218 (+77/-70)	1070 (+74/-78)	1051 (+29/-34)	1044 (+90/-78)
SDXL-turbo	1039 (+45/-46)	987 (+57/-71)	980 (+36/-41)	945 (+89/-136)	1018 (+53/-56)	1027 (+69/-71)	1033 (+36/-37)	1053 (+79/-80)
SD3	1033 (+48/-41)	1003 (+76/-71)	1002 (+33/-35)	996 (+58/-86)	976 (+54/-47)	976 (+68/-58)	963 (+35/-32)	959 (+57/-70)
SDXL	1015 (+39/-36)	1033 (+74/-113)	1050 (+39/-31)	1089 (+109/-85)	980 (+54/-52)	1060 (+73/-68)	1035 (+32/-32)	997 (+80/-71)
HDiT	994 (+32/-43)	946 (+70/-59)	1031 (+33/-35)	988 (+70/-76)	1034 (+67/-70)	1015 (+60/-58)	1019 (+33/-38)	953 (+80/-77)
PixArt	990 (+43/-65)	1027 (+69/-62)	1082 (+33/-31)	1050 (+78/-67)	1030 (+59/-57)	1052 (+71/-70)	1036 (+36/-35)	1075 (+72/-68)
Kandinsky3	961 (+42/-48)	1059 (+81/-63)	1014 (+38/-39)	1005 (+87/-60)	999 (+61/-87)	992 (+51/-71)	1063 (+40/-30)	992 (+64/-97)
Retrieval	960 (+50/-48)	953 (+90/-83)	940 (+39/-47)	990 (+107/-104)	890 (+62/-62)	1023 (+111/-63)	947 (+37/-45)	1030 (+81/-90)
Openjourney	941 (+45/-41)	907 (+73/-66)	885 (+37/-49)	902 (+73/-102)	928 (+79/-70)	906 (+67/-70)	874 (+42/-42)	988 (+72/-73)
SD1.5	900 (+46/-59)	914 (+72/-61)	889 (+38/-36)	942 (+76/-67)	891 (+58/-70)	933 (+68/-79)	904 (+30/-34)	857 (+61/-81)

Table 5: ELO score for Human Preferences for subsets with definition in input.

Model	**Ground Truth**				**Predicted**			
	Easy	**Hypo**	**Hyper**	**Mix**	**P-Easy**	**P-Hypo**	**P-Hyper**	**P-Mix**
Playground	1044 (+46/-33)	1044 (+70/-68)	1043 (+28/-30)	1006 (+66/-67)	1006 (+62/-55)	972 (+76/-55)	1039 (+32/-29)	973 (+61/-69)
PixArt	940 (+35/-41)	1036 (+64/-74)	1035 (+36/-30)	1138 (+84/-84)	1037 (+50/-46)	954 (+68/-94)	1020 (+26/-31)	1041 (+74/-75)
Kandinsky3	979 (+47/-33)	1060 (+97/-62)	1027 (+39/-32)	1034 (+63/-86)	978 (+58/-49)	1016 (+56/-72)	1045 (+43/-37)	998 (+73/-80)
SD3	1048 (+37/-54)	967 (+67/-69)	1026 (+32/-31)	1074 (+80/-76)	1044 (+69/-51)	970 (+70/-52)	996 (+27/-32)	951 (+68/-76)
SDXL	1022 (+46/-41)	948 (+54/-52)	1017 (+39/-27)	939 (+114/-83)	1016 (+44/-49)	1026 (+92/-60)	985 (+30/-24)	1125 (+75/-75)
FLUX	1011 (+51/-46)	1015 (+75/-100)	1008 (+42/-43)	1012 (+92/-84)	1144 (+75/-59)	1102 (+79/-64)	1043 (+32/-26)	941 (+64/-83)
HDiT	964 (+42/-41)	988 (+61/-87)	1001 (+28/-34)	961 (+92/-93)	1040 (+48/-41)	949 (+69/-70)	1001 (+36/-34)	983 (+63/-88)
Retrieval	1041 (+49/-49)	1027 (+79/-72)	995 (+32/-29)	1051 (+71/-83)	893 (+61/-57)	1093 (+86/-73)	976 (+37/-38)	1027 (+96/-84)
SDXL-turbo	992 (+48/-41)	989 (+60/-65)	984 (+37/-37)	986 (+90/-88)	1010 (+40/-56)	1033 (+73/-68)	1053 (+37/-23)	1049 (+64/-66)
DeepFloyd	1000 (+37/-40)	969 (+62/-54)	970 (+35/-39)	1037 (+76/-78)	959 (+40/-56)	1013 (+64/-86)	979 (+34/-31)	963 (+57/-82)
SD1.5	968 (+52/-56)	991 (+73/-69)	958 (+36/-31)	918 (+85/-79)	935 (+48/-51)	947 (+54/-65)	948 (+25/-36)	970 (+71/-63)
Openjourney	983 (+48/-43)	958 (+63/-52)	930 (+32/-42)	838 (+67/-96)	931 (+63/-53)	918 (+56/-63)	908 (+33/-38)	973 (+83/-95)

Table 6: ELO score for Human Preferences for subsets with no definition in input.

Model	Inception Score	FID
DeepFloyd	19.6	62
Kandinsky3	19.4	64
PixArt	19.8	73
Playground	20.9	71
Openjourney	15.4	68
SD1.5	18.0	59
SDXL-turbo	10.9	89
SD3	21.2	63
HDiT	18.2	67
SDXL	19.1	63
FLUX	20.9	68
Retrieval	19.1	-

Table 7: FID and IS metrics for different models on the full dataset without repetitions

Model	**IS**		**FID**	
	def	**no_def**	**def**	**no_def**
DeepFloyd	19.6	12.1	62	131
Kandinsky3	19.4	18.2	64	75
PixArt	19.8	18.8	73	73
Playground	20.9	20.0	71	74
Openjourney	15.4	13.9	68	73
SD1.5	18.0	17.5	59	60
SDXL-turbo	10.9	12.1	89	65
SD3	21.2	23.5	63	65
HDiT	18.2	20.2	67	85
SDXL	19.1	19.6	63	68
FLUX	20.9	22.0	68	72

Table 8: Comparing FID and IS for datasets with and without definition

Model	**Ground Truth**				**Predicted**			
	Hypo	**Hyper**	**Mix**	**Easy**	**Hypo**	**Hyper**	**Mix**	**Easy**
DeepFloyd	8.2	9.3	6.6	12.9	8.3	11.3	6.8	7.3
Kandinsky-3	7.4	10.3	6.6	12.8	7.8	11.7	7.0	8.4
PixArt	7.6	10.5	6.6	13.5	7.6	11.2	7.1	8.6
Playground	8.6	11.0	7.0	13.3	8.0	12.0	7.8	8.3
Openjourney	6.7	8.2	6.3	12.5	6.9	9.0	6.4	7.0
SD1.5	7.1	9.0	6.9	12.9	7.4	9.5	6.6	8.1
SDXL-turbo	5.2	6.7	4.7	9.9	5.3	6.8	5.1	6.1
SD3	8.4	9.5	7.2	13.3	8.1	12.0	7.3	8.8
HDiT	8.0	10.1	6.8	11.2	7.3	11.8	7.0	7.7
SDXL	7.6	10.4	7.1	12.8	7.5	11.4	7.3	8.1
FLUX	8.3	10.5	7.5	12.9	8.3	12.7	7.2	8.0
Retrieval	7.8	10.5	6.7	11.4	8.5	12.7	6.7	8.2

Table 9: Inception Score per subsets with definitions

Model	**Ground Truth**				**Predicted**			
	Hypo	**Hyper**	**Mix**	**Easy**	**Hypo**	**Hyper**	**Mix**	**Easy**
DeepFloyd	195	134	191	128	220	219	147	193
Kandinsky3	203	134	197	127	229	224	155	191
PixArt	203	143	191	134	229	230	163	203
Playground	198	143	188	130	234	225	163	196
Openjourney	200	145	197	127	225	228	159	198
SD1.5	192	135	192	125	229	221	154	186
SDXL-turbo	207	158	211	146	235	226	170	203
SD3	193	135	193	133	225	218	153	184
HDiT	201	141	187	126	226	225	160	198
SDXL	192	133	199	129	230	223	163	191
FLUX	163	132	186	139	165	115	182	171

Table 10: Fréchet Inception Distance Score per subsets with definitions

Model	**Ground Truth**				**Predicted**			
	Easy	**Hypo**	**Hyper**	**Mix**	**P-Easy**	**P-Hypo**	**P-Hyper**	**P-Mix**
HDiT	0.65	0.60	0.61	0.61	0.57	0.59	0.59	0.60
Retrieval	0.63	0.56	0.57	0.60	0.54	0.57	0.56	0.60
Kandinsky3	0.66	0.61	0.61	0.62	0.58	0.60	0.59	0.61
Openjourney	0.63	0.59	0.59	0.60	0.57	0.58	0.59	0.59
DeepFloyd	0.64	0.60	0.60	0.62	0.57	0.59	0.60	0.60
SDXL-turbo	0.67	0.62	0.62	0.63	0.59	0.61	0.60	0.61
Playground	0.66	0.60	0.61	0.61	0.57	0.59	0.59	0.60
SDXL	0.66	0.60	0.61	0.61	0.58	0.59	0.59	0.60
PixArt	0.65	0.60	0.60	0.62	0.57	0.59	0.59	0.61
SD3	0.66	0.61	0.61	0.62	0.57	0.60	0.60	0.60
SD1.5	0.64	0.60	0.60	0.61	0.57	0.58	0.60	0.59
FLUX	0.70	0.62	0.61	0.63	0.57	0.59	0.59	0.6

Table 11: Hypernym CLIPScore Across Different Subsets

Model	**Ground Truth**				**Predicted**			
	Easy	**Hypo**	**Hyper**	**Mix**	**Easy**	**Hypo**	**Hyper**	**Mix**
HDiT	0.73	0.66	0.67	0.68	0.72	0.67	0.68	0.68
Retrieval	0.68	0.60	0.62	0.66	0.63	0.63	0.63	0.69
Kandinsky3	0.73	0.67	0.67	0.69	0.73	0.68	0.68	0.69
Openjourney	0.71	0.66	0.66	0.68	0.71	0.67	0.66	0.69
DeepFloyd	0.71	0.67	0.66	0.69	0.70	0.67	0.66	0.69
SDXL-turbo	0.76	0.71	0.71	0.73	0.75	0.72	0.71	0.74
Playground	0.74	0.67	0.68	0.70	0.72	0.69	0.68	0.70
SDXL	0.73	0.67	0.67	0.69	0.73	0.69	0.68	0.70
PixArt	0.72	0.66	0.67	0.69	0.72	0.67	0.67	0.68
SD3	0.73	0.68	0.67	0.70	0.72	0.69	0.68	0.70
SD1.5	0.73	0.68	0.67	0.70	0.72	0.69	0.68	0.70
FLUX	0.71	0.65	0.66	0.68	0.72	0.68	0.67	0.69

Table 12: Lemma CLIPScore Across Different Subsets

Model	**CLIP-Score**	**Hypernym CLIP-Score**	**Cohyponym CLIP-Score**	**Specificity**
HDiT	0.69	0.60	0.58	1.2
Retrieval	0.64	0.57	0.56	1.16
Kandinsky3	0.69	0.61	0.59	1.19
Openjourney	0.68	0.59	0.57	1.2
DeepFloyd	0.68	0.60	0.58	1.18
SDXL-turbo	**0.72**	**0.62**	**0.60**	1.23
Playground	0.70	0.60	0.58	1.22
SDXL	0.69	0.60	0.58	1.2
PixArt	0.68	0.60	0.58	1.19
SD3	0.70	0.60	0.58	1.21
SD1.5	0.69	0.59	0.57	**1.23**
FLUX	0.68	0.61	0.58	1.17

Table 13: Summary of CLIPscore Metrics Across Models

Model	**Ground Truth**				**Predicted**			
	Easy	**Hypo**	**Hyper**	**Mix**	**P-Easy**	**P-Hypo**	**P-Hyper**	**P-Mix**
HDiT	1.21	1.14	1.15	1.16	1.34	1.18	1.18	1.18
Retrieval	1.17	1.11	1.13	1.14	1.24	1.15	1.15	1.18
Kandinsky3	1.21	1.14	1.15	1.16	1.32	1.18	1.19	1.18
Openjourney	1.22	1.16	1.15	1.17	1.32	1.18	1.18	1.21
DeepFloyd	1.18	1.16	1.14	1.15	1.29	1.16	1.16	1.18
SDXL-turbo	1.23	1.18	1.18	1.20	1.34	1.22	1.22	1.24
Playground	1.24	1.16	1.17	1.20	1.34	1.21	1.20	1.21
SDXL	1.22	1.15	1.15	1.18	1.33	1.20	1.19	1.20
PixArt	1.20	1.14	1.15	1.16	1.34	1.17	1.18	1.17
SD3	1.23	1.17	1.16	1.19	1.34	1.20	1.20	1.20
SD1.5	1.24	1.19	1.18	1.20	1.34	1.22	1.21	1.23
FLUX	1.14	1.10	1.12	1.13	1.32	1.18	1.18	1.20

Table 14: Specificity Scores Across Different Models and Subsets

Model	Ground Truth				Predicted			
	Easy	Hypo	Hyper	Mix	P-Easy	P-Hypo	P-Hyper	P-Mix
HDiT	0.61	0.59	0.58	0.60	0.54	0.57	0.58	0.58
Retrieval	0.59	0.55	0.55	0.59	0.51	0.56	0.55	0.58
Kandinsky3	0.61	0.59	0.59	0.61	0.55	0.58	0.59	0.59
Openjourney	0.59	0.58	0.57	0.59	0.54	0.57	0.57	0.57
DeepFloyd	0.61	0.58	0.58	0.61	0.55	0.57	0.58	0.59
SDXL-turbo	0.62	0.60	0.60	0.62	0.56	0.59	0.60	0.60
Playground	0.60	0.58	0.58	0.60	0.54	0.57	0.58	0.58
SDXL	0.61	0.58	0.58	0.60	0.55	0.58	0.58	0.60
PixArt	0.60	0.59	0.58	0.61	0.54	0.57	0.58	0.59
SD3	0.61	0.59	0.58	0.60	0.54	0.58	0.58	0.59
SD1.5	0.60	0.58	0.57	0.60	0.54	0.56	0.57	0.57
FLUX	0.63	0.59	0.59	0.61	0.54	0.57	0.57	0.58

Table 15: Cohyponym CLIPScore Across Different Subsets

	SDXL-turbo	Retrieval	SD1.5	HDiT	Playground	Openjourney	Kandinsky3	SDXL	PixArt	DeepFloyd	SD3	FLUX
SDXL-turbo	0	0	0	0.003	0	0	0.036	0	0	0.027	0.029	0
Retrieval	0	0	0	0	0	0	0	0	0	0	0	0
SD1.5	0	0	0	0	0	0.037	0	0	0	0	0	0
HDiT	0.003	0	0	0	0	0	0	0	0	0	0.702	0
Playground	0	0	0	0	0	0	0	0	0	0	0	0
Openjourney	0	0	0.037	0	0	0	0	0	0	0	0	0
Kandinsky3	0.036	0	0	0	0	0	0	0	0.167	0.95	0	0
SDXL	0	0	0	0	0	0	0	0	0	0	0	0
PixArt	0	0	0	0	0	0	0.167	0	0	0.14	0	0
DeepFloyd	0.027	0	0	0	0	0	0.95	0	0.14	0	0	0
SD3	0.029	0	0	0.702	0	0	0	0	0	0	0	0
FLUX	0	0	0	0	0	0	0	0	0	0	0	0

Table 16: P-value of Mann-Whitney mean differences test in rewards for models. Values below 0.000 are marked as 0. To identify the side of difference, refer to the violin plot in Figure 10

I Models' Mistake Analysis

This analysis is made for generation without definitions.

All models struggle with depicting

a. abstract concepts;

b. nonfrequent and specific words (”orifice.n.01” with the lemma ”rima”);

c. notions of people with specific functional role (”holder.n.02” with the lemma ”holder”, for example).

Abstract concepts are handled with the following:

1. Text in images (although not all models succeed in writing);

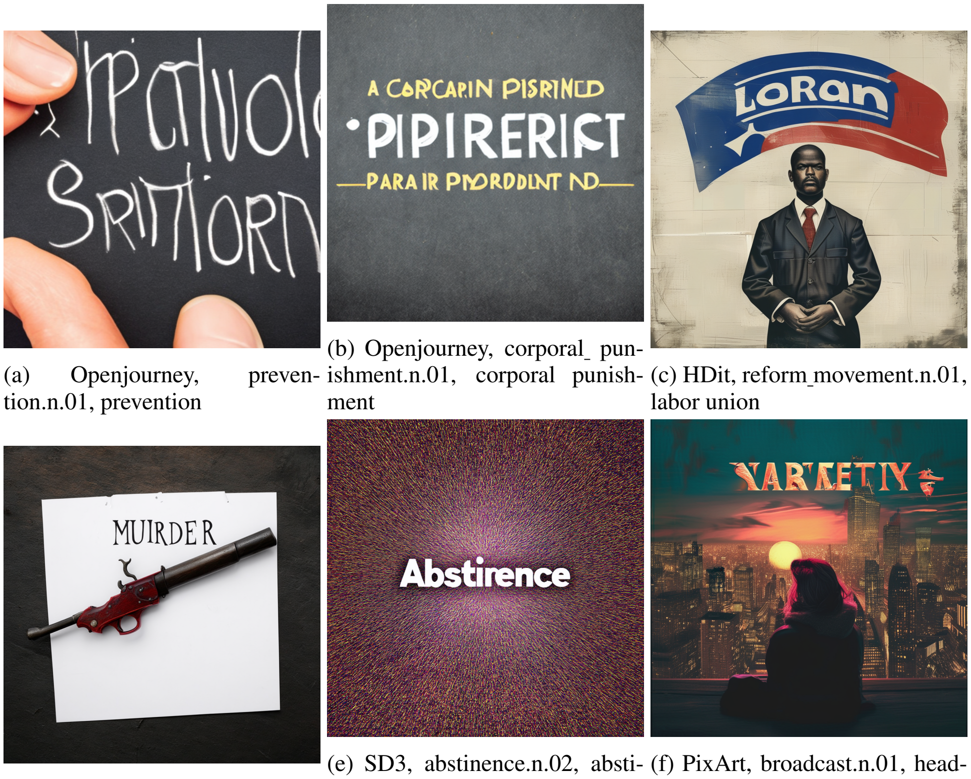

(a) Openjourney, prevention.n.01, prevention

(b) Openjourney, corporal_ punishment.n.01, corporal punishment

(c) HDit, reform_movement.n.01, labor union

(d) SD3, murder.n.01, murder

(e) SD3, abstinence.n.02, abstinence

(f) PixArt, broadcast.n.01, headline

Figure 13: Text in images

2. Abstract images;

Other unwanted behaviors for the purposes of illustrating taxonomies include

1. Generating playing cards for the concepts (most seen in Openjourney, also present in SD1.5);
2. Abstract ornamental circles (also most found in Openjourne, and some in SD1.5).
3. Depicturing monsters when facing rare animal names (seen in Kandinsky3).

Most importantly, models struggle closer to the leaves of a taxonomy: they tend to create an image of a parent concept without necessary features of the child (see figure 21).

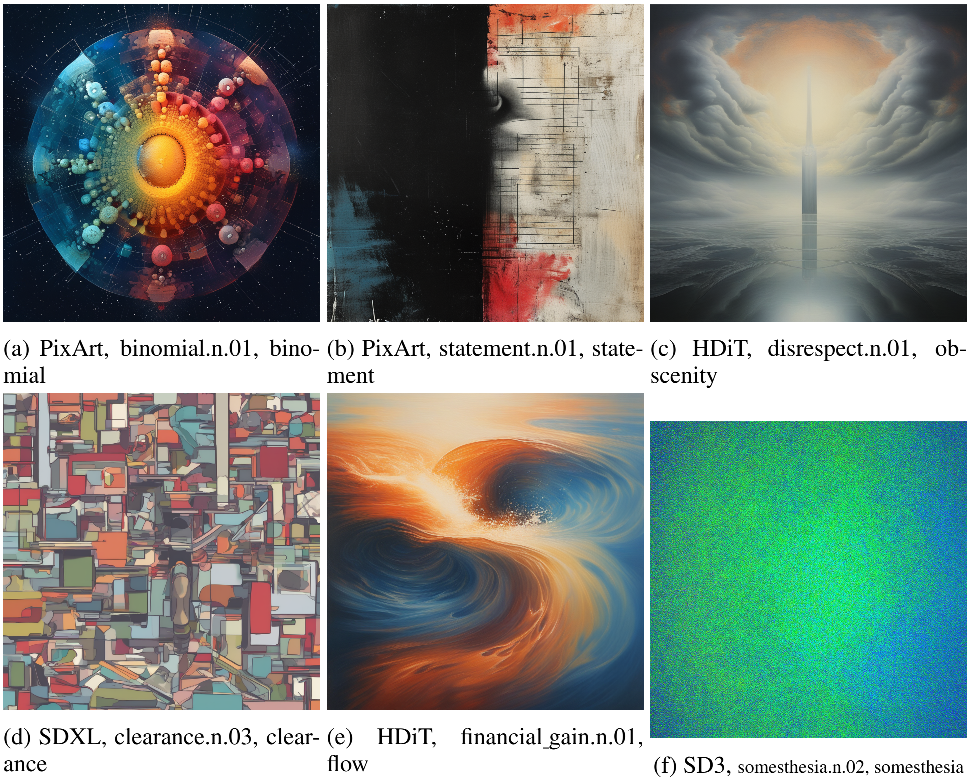

(a) PixArt, binomial.n.01, binomial

(b) PixArt, statement.n.01, statement

(c) HDiT, disrespect.n.01, obscenity

(d) SDXL, clearance.n.03, clearance

(e) HDiT, financial_gain.n.01, flow

(f) SD3, somesthesia.n.02, somesthesia

Figure 14: Abstract images

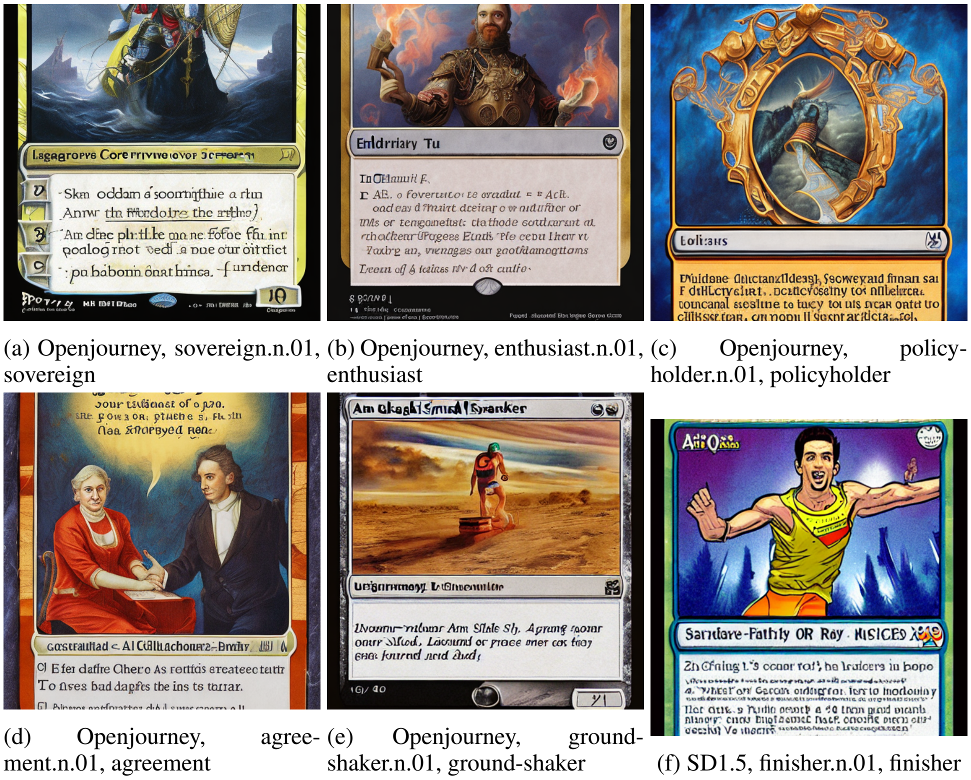

(a) Openjourney, sovereign.n.01, sovereign

(b) Openjourney, enthusiast.n.01, enthusiast

(c) Openjourney, policyholder.n.01, policyholder

(d) Openjourney, agreement.n.01, agreement

(e) Openjourney, ground-shaker.n.01, ground-shaker

(f) SD1.5, finisher.n.01, finisher

Figure 15: Playing cards in Openjourney and SD1.5

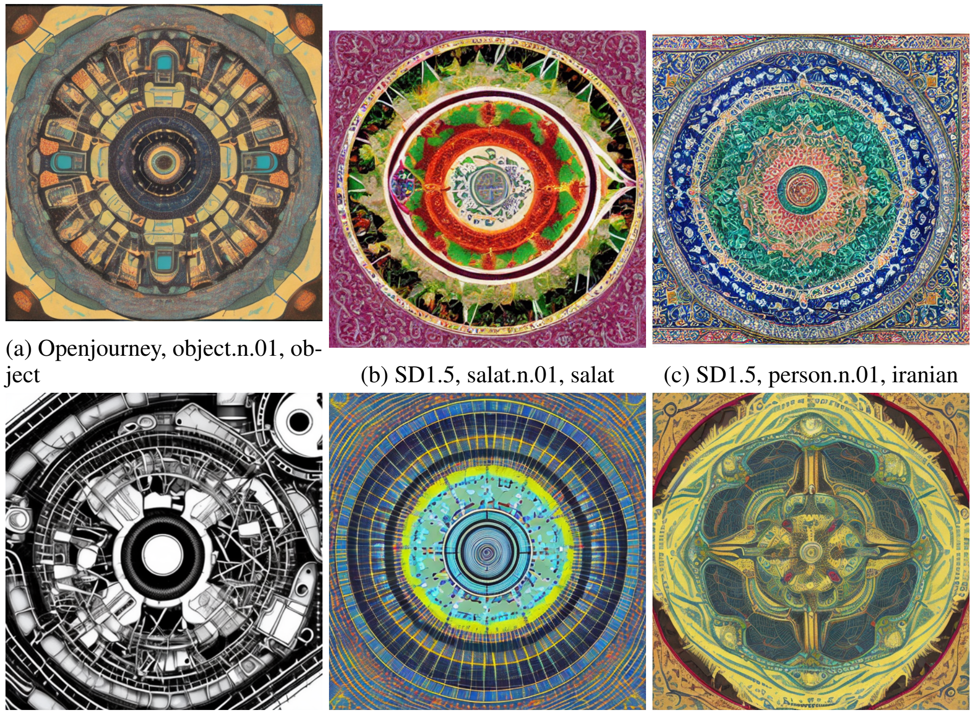

(a) Openjourney, object.n.01, object

(b) SD1.5, salat.n.01, salat

(c) SD1.5, person.n.01, iranian

(d) Openjourney, engineering.n.03, engineering

(e) Openjourney, lingtpen.n.01, light pen

(f) Openjourney, organization.n.01, baptist association

Figure 16: Abstract ornamental circles

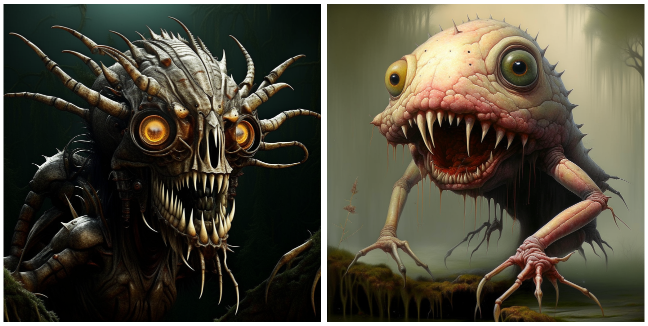

(a) Kandinsky3, acanthocephalan.n.01, acanthocephalan

(b) Kandinsky3, gelechiid.n.01, gelechiid

Figure 17: Monsters for rare animal names in Kandinsky

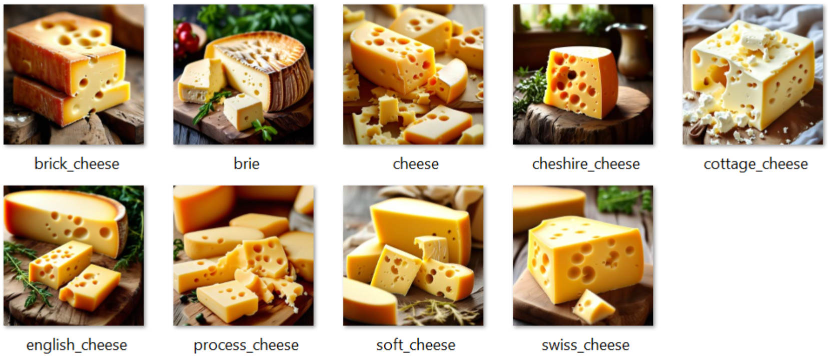

Figure 18: PixArt images for ”cheese” and some of its hyponyms

J Demonstration System Examples

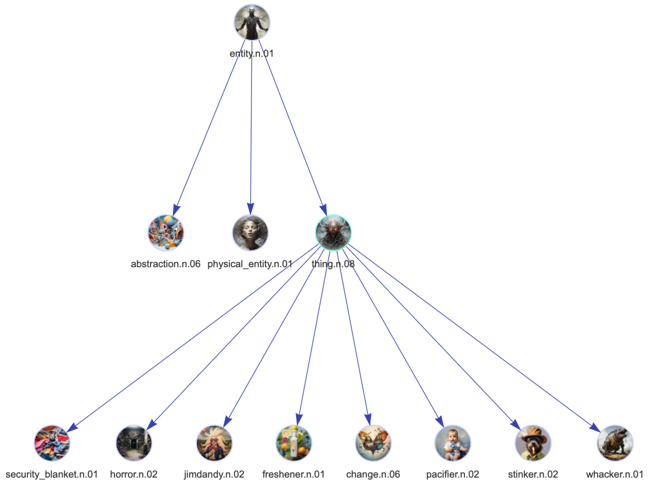

Figure 19: Subgraph starting from the root node "entity.n.01". Images are generated with the best TTI model.

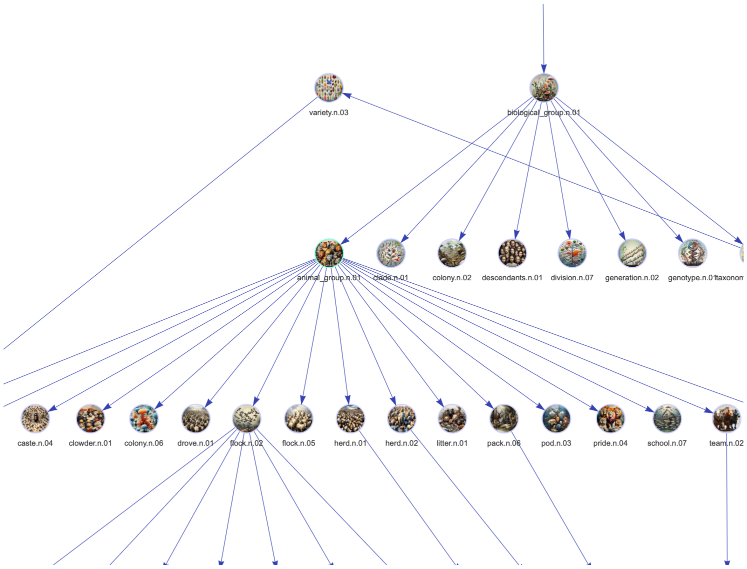

Figure 20: Subgraph starting from the node "biological_group.n.01". Images are generated with the best TTI model.

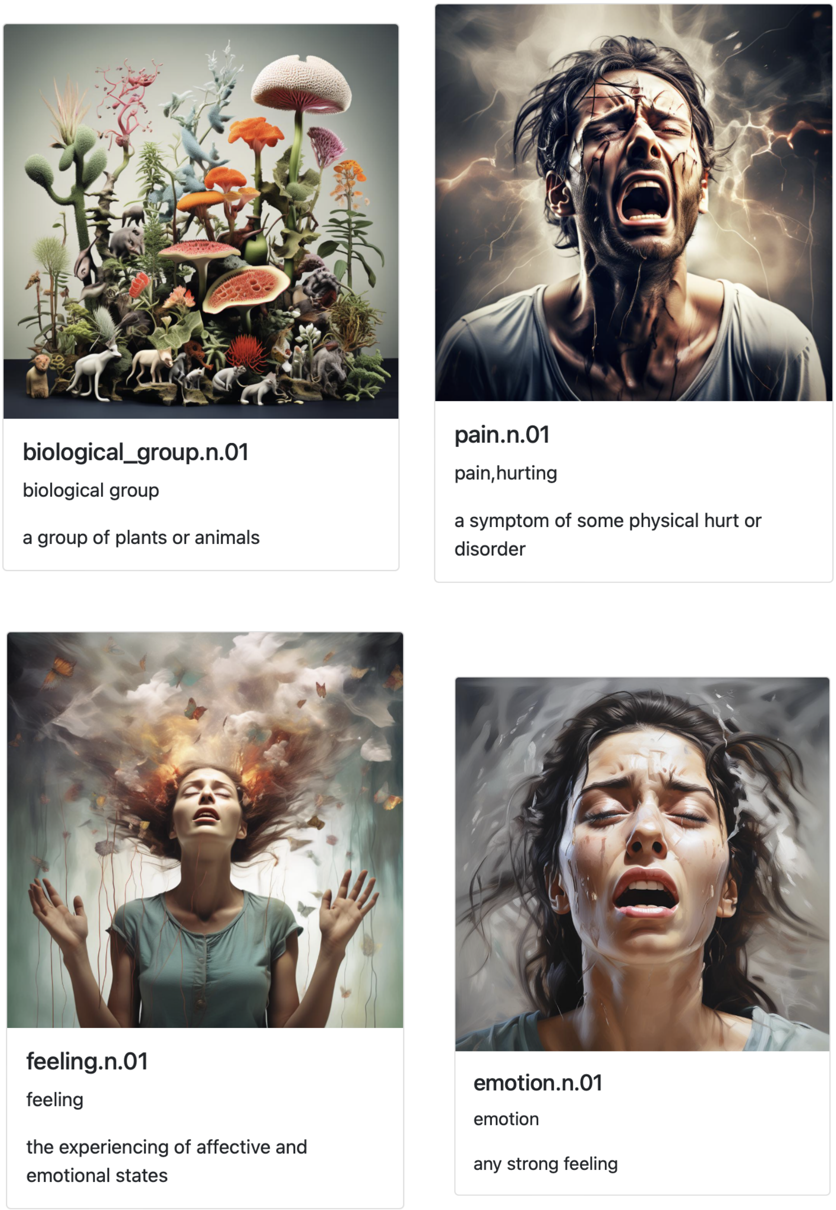

biological_group.n.01

biological group

a group of plants or animals

pain.n.01

pain,hurting

a symptom of some physical hurt or disorder

feeling.n.01

feeling

the experiencing of affective and emotional states

emotion.n.01

emotion

any strong feeling

Figure 21: Node descriptions from the demonstration system with the generated image using the best-performing model.

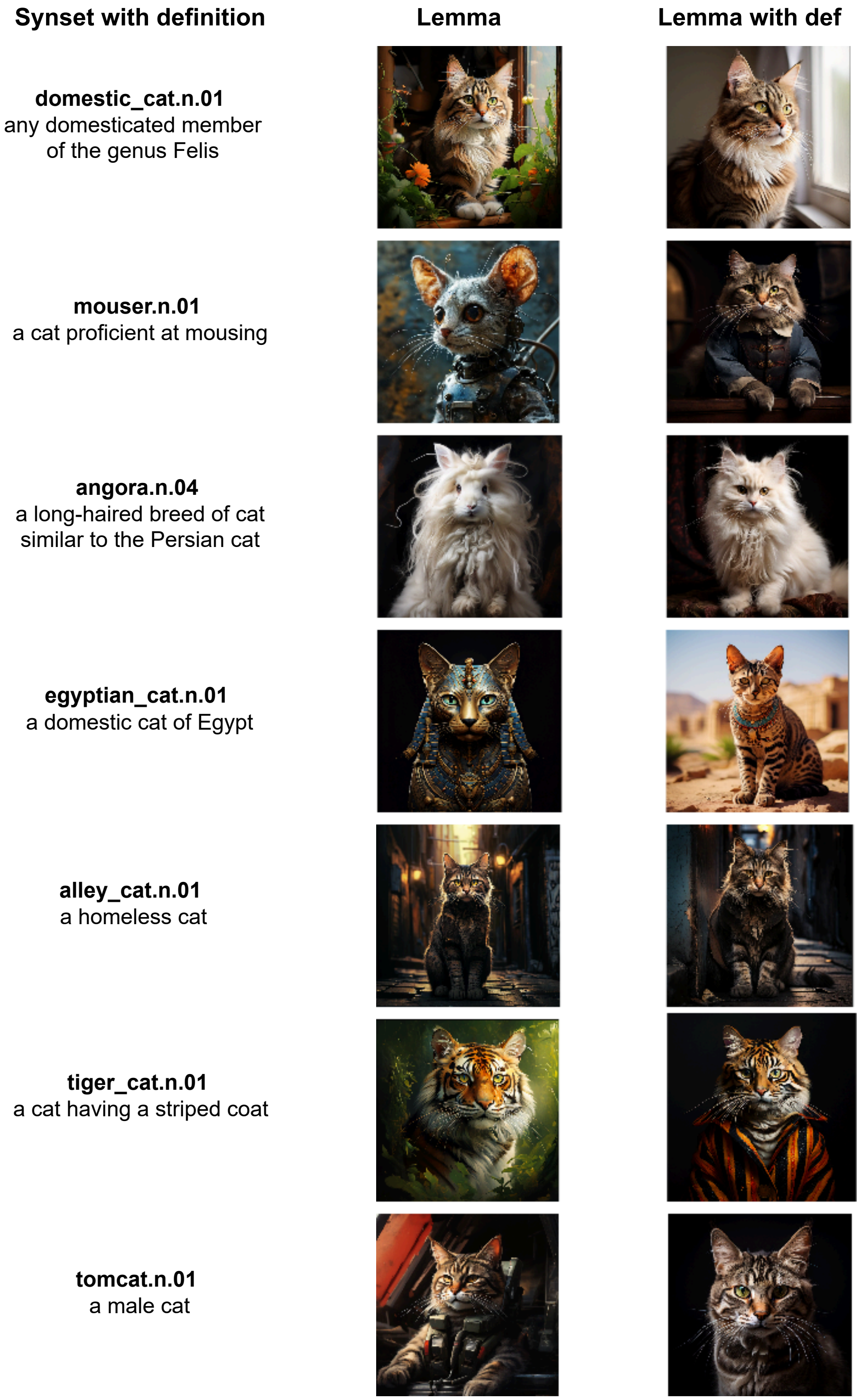

Figure 22: Examples of the generations for the 'domestic_cat.n.01' hyponyms using playground-v2.5-1024px-aesthetic model. The examples illustrate common confusion patterns without introducing an additional labeling step: mouser has features from "Mouser Electronics" and a mouse; Angora is mixed within a rabbit and has wool patterns; tiger cat either looks like a tiger or has a striped coat; tomcat is confused with aircraft and has made a cat a military pilot.